Simocetus rayi (Odontoceti: Simocetidae, New Family): A Bizarre New Archaic Oligocene Dolphin from the Eastern North Pacific

R. Ewan Fordyce

ABSTRACT

Simocetus rayi (new genus, new species) is based upon a skull and mandible of a small archaic dolphin (Cetacea: Odontoceti) from the upper Oligocene Alsea Formation of Oregon, bordering the northeast Pacific. The species shows many primitive features reminiscent of the archaic odontocete family Agorophiidae: the cheek teeth appear nonpolydont, the nares and premaxillary sac fossae lie anteriorly, the orbit and facial fossa are elevated above the level of the rostrum, the ascending processes of premaxillae are narrow and long, the supraorbital processes of the maxillae are narrow, the intertemporal constriction is prominent, and the pterygoid sinus fossae are restricted to the basicranium. These features are consistent with a basal position among the odontocetes, but they do not justify placement in the paraphyletic- and probably polyphyletic-grade family Agorophiidae. *Simocetus rayi* shows some unusual autapomorphies (toothless premaxillae, anterior of rostrum and mandible downturned) that exclude it from described taxa of odontocetes, and for this reason it is placed in a new and currently monotypic family, Simocetidae. Broader relationships are uncertain; some cranial features hint at affinities with Eurhinodelphinidae. For now, *S. rayi* is regarded as a specialized archaic odon-tocete that lies stemward (more basal) to all extant groups of Odontoceti (namely, Physeteroidea, Ziphiidae, Platanistoidea, and Delphinida).

Simocetus rayi was perhaps a bottom feeder that preyed through suction feeding on soft-bodied invertebrates. The inferred presence of nasal turbinals and a vomeronasal organ contrasts with the situation in living odontocetes. Features of the face and basicranium point to echolocation abilities comparable to those of extant Odontoceti. *Simocetus rayi* and other contemporaneous archaic odontocetes from Oregon and Washington indicate that odontocetes were taxonomically and ecologically diverse by the late Oligocene.

R. Ewan Fordyce, Department of Geology, University of Otago, Dunedin, New Zealand; and Research Associate, Department of Vertebrate Zoology, National Museum of Natural History, Smithsonian Institution, Washington, D.C. 20560-0121, United States.

Introduction

Odontocetes, which include toothed whales, dolphins, and porpoises, have an extensive fossil record from the late Oligocene to Holocene. In the last decade, sound progress has been made in understanding the relationships between many living groups, particularly those with a Miocene to Holocene record (Muizon, 1987, 1988a, 1988b, 1991). In contrast, the morphology and relationships of archaic odontocetes—heterodont dolphins that retain an intertemporal constriction—are understood poorly. The so-called primitive odontocetes have nonetheless been pivotal in helping develop basic concepts of odontocete evolution. Indeed, one species, *Agorophius pygmaeus* (Müller, 1849), is the basis for the family Agorophiidae Abel, 1913, from which, according to many authors, later odontocetes evolved. This article describes and discusses a new species and new genus of archaic odontocete that has been mentioned previously (Muizon, 1991:303) as a species of Agorophiidae, but that is herein placed in a new group, Simocetidae. The fossil, USNM 256517, shows many details of cranial structure not recorded previously for archaic odontocetes. It is the first archaic odontocete from the northeastern Pacific margin to be described formally. Although the species shows a wide range of primitive features, consistent with its late Oligocene age and rather basal position in the Odontoceti, it is too specialized, particularly in terms of feeding apparatus, to have been directly ancestral to any other described odontocete.

Specimen USNM 256517 is one of several hundred fossil vertebrates assembled by the late Douglas R. Emlong, which now constitute the Emlong collection (Ray, 1977, 1980; Domning et al., 1986) in the National Museum of Natural History. The Emlong collection comprises fossils from a thin sequence of marine Oligocene and Neogene rocks along the eastern coast of the North Pacific Ocean, mainly from Oregon and Washington. Other unnamed species of archaic odontocete are repre-

sented by undescribed specimens in the Emlong collection; mentioned below are USNM 205491 ("non-squalodontid odontocete" of Whitmore and Sanders, 1977, fig. 2b, from Alsea Formation, Oregon), USNM 243979 ("non-squalodontid odontocete" of Whitmore and Sanders, 1977, fig. 2a, from ?Pysht Formation, Washington), and USNM 299482 (?Pysht Formation, Washington), all of which are of Oligocene age.

Descriptions below are based upon the right or left side, whichever is more nearly complete. Some comparisons are offered in the descriptive text to clarify homologies, but fuller systematic comparisons follow the description. Absences are noted for some cranial features that are present in archaeocete cetaceans but are enigmatic or missing in most odontocetes. Unreferenced statements about cetacean anatomy are based upon personal observations. Nomenclature follows that used by Kellogg (1936), Kasuya (1973), Fordyce (1994), and others, with modifications and synonyms (following Sisson and Grossman, 1953; Davis, 1964; Novacek, 1986; Evans, 1993) to better identify cetacean homologs with those of other mammals. The few postcranial elements are rather uninformative and are not described.

Line diagrams are from 35 mm photographs (Asahi Pentax camera, 50 mm macro lens) and are not corrected for parallax. Illustrations are by the author.

F.V. Grady carried out most of the preparation using mechanical tools. The author prepared fine details under a low-power binocular microscope using pneumatic scribe and an air-abrasive unit. Much of the matrix is a leached (formerly calcareous) mudstone that bonds tightly to bone, and still obscures some sutures and foramina.

ABBREVIATIONS.—The following abbreviations are used:

AMNH	Departments of Mammalogy and of Vertebrate Paleontology, American Museum of Natural History, New York
MCZ	Museum of Comparative Zoology, Harvard University, Cambridge, Massachusetts
MNHN	Muséum Nationale d'Histoire Naturelle, Paris
OU	Geology Museum, University of Otago, Dunedin, New Zealand
USGS	United States Geological Survey
USNM	Collections of the National Museum of Natural History, Smithsonian Institution, Washington, D.C., including those of the former United States National Museum

ACKNOWLEDGMENTS.—Work was started during the tenure of a Smithsonian Postdoctoral Fellowship in the Department of Paleobiology from early 1979 to mid-1980 and was continued with support from Smithsonian short-term visiting fellowships. The University of Otago supported visits to the Smithsonian Institution in 1984, 1988–1989, 1994, and 1996. I am indebted to Frank C. Whitmore, Jr., for his valuable guidance and advice over the years. I gratefully thank Clayton E. Ray for facilitating diverse aspects of this study, and Frederick V. Grady for preparation. Lawrence G. Barnes, Hiroto Ichishima, Richard Köhler, James G. Mead, Mark D. Uhen, and Frank C. Whitmore, Jr., reviewed different versions of the manuscript. Barnes, Mead, Whitmore, and Christian de Muizon also provided fruitful ongoing discussion of cetacean systematics. Lawrence G. Barnes, David J. Bohaska, Andrew P. Currant, John T. Darby, Anton van Helden, Jerry J. Hooker, James G. Mead, Clayton E. Ray, Thomas H. Rich, Richard H. Tedford, and Albert E. Sanders kindly arranged access to specimens studied as part of this work.

Class MAMMALIA

Order CETACEA

Suborder ODONTOCETI

DIAGNOSIS.—Odontoceti are recognized herein as Cetacea with the following combination of osteological features: supraorbital process of maxilla telescoped posteriorly over frontal; one or more dorsal infraorbital (=maxillary) foramina open posteriorly in supraorbital process of maxilla; premaxillary sac fossa, premaxillary sulci, and premaxillary foramen (or foramina) present; infraorbital process of maxilla reduced; posteriormost teeth inserted anterior to antorbital notch; orbitotemporal crest displaced posterodorsally relative to postorbital ridge and partly roofing temporal fossa; distinct antorbital notch faces anteriorly to anterolaterally; pterygoid hamulus partly excavated for the pterygoid sinus system; ossified mesethmoid present between bony nares; and parietal and squamosal dorsointernally override periotic to occlude the cranial hiatus.

REMARKS.—These features are seen in or inferred for *S. rayi*. They are modified in some other odontocetes. Many of the facial features listed appear to be linked to the presence of a posteriorly displaced and hypertrophied maxillo-naso-labialis (nasofacial) muscular complex, and thus to the ability to generate high-frequency sound that might be used in echolocation. See "Discussion," below.

Superfamily Incertae Sedis

SIMOCETIDAE, new family

DIAGNOSIS.—As for *Simocetus rayi,* at present the only included species; see remarks under species diagnosis.

TYPE GENUS.—*Simocetus* new genus.

INCLUDED GENERA.—*Simocetus* new genus only.

Simocetus, new genus

ETYMOLOGY.—From *simus,* pug-nosed, and *cetus,* whale (Greek). In allusion to the prominent medial "snout" posterior to the external nares.

DIAGNOSIS.—As for *Simocetus rayi,* at present the only included species; see remarks under species diagnosis.

TYPE SPECIES.—*Simocetus rayi* new species.

INCLUDED SPECIES.—*Simocetus rayi* only.

Simocetus rayi, new species

Agorophius sp., Muizon, 1991:303.

HYPODIGM.—USNM 256517 (Emlong collection number

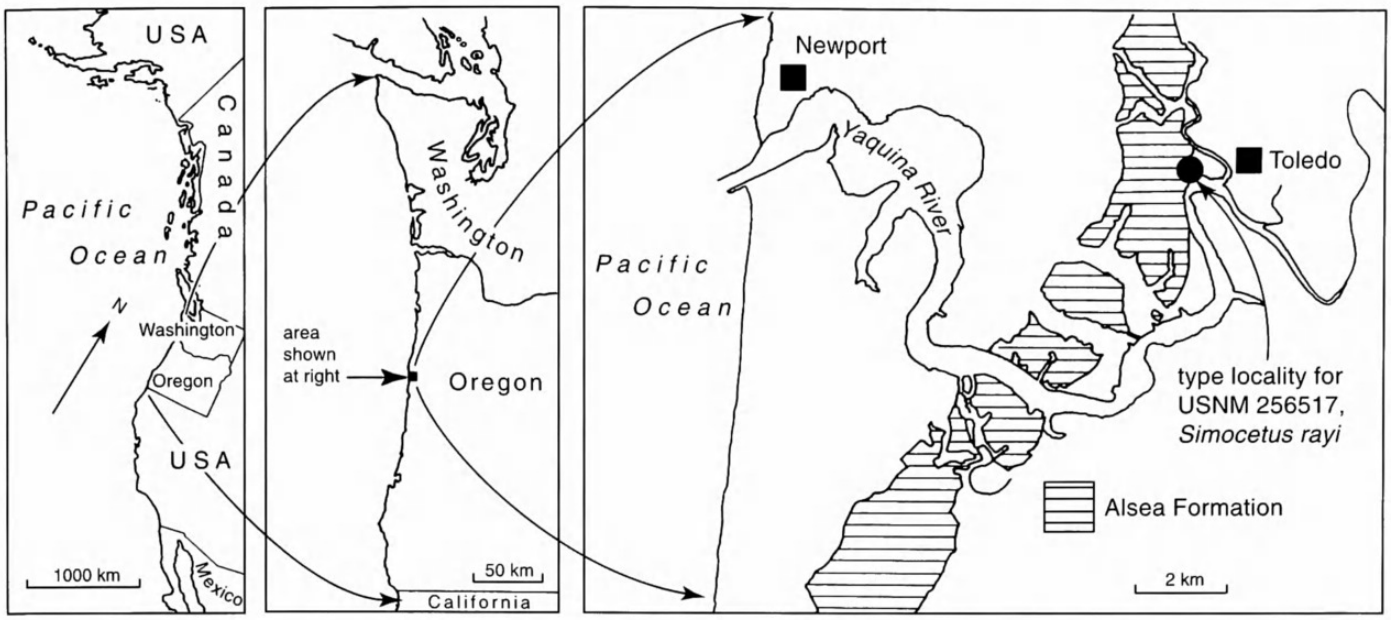

FIGURE 1.—Locality map of Pacific Northwest. The detailed map is based upon Snavely et al. (1975, 1976).

E77-32), holotype, only. Almost-complete skull, right periotic in place on skull, incomplete right mandible, three anterior teeth, 10 cheek teeth (four in place in rostrum, four in place in mandible), two incomplete presumed lumbar vertebrae, one chevron, eight or more incomplete ribs. Collected by D.R. Emlong, 3 August 1977.

DIAGNOSIS.—Small odontocete. More primitive than described species of Squalodontidae, Waipatiidae, Squalodelphinidae, Platanistidae, Dalpiazinidae, Eoplatanistidae, Eurhinodelphinidae, Lipotidae, Pontoporiidae, Iniidae, Albireonidae, Kentriodontidae, Delphinidae, Phocoenidae, Monodontidae, Ziphiidae, Physeteridae, and Kogiidae. Primitive features as follows: premaxillary sac fossa located well forward on rostrum; lateral margin of rostrum (rostral base) located well ventral to level of elevated roof of orbit; rostrum with well-developed fossa for nasofrontal muscles; ventral infraorbital foramen and sphenopalatine foramen opening in a large infundibulum in anterior wall of orbit; external nares open well forward of level of antorbital notch; median facial elements (nasals plus frontals) form an elongate "snout"; multiple supraorbital foramina open on frontal; elongate palatine forms much of palate; and parietals and interparietal form elongate intertemporal constriction.

Similar to *Agorophius pygmaeus* (Agorophiidae) only in plesiomorphic features including heterodont teeth; premaxillary sac fossa and associated foramina and sulci lying well forward on rostrum; lateral margin of rostrum (rostral base) lying ventral to level of elevated roof of orbit; and parietals contributing to an elongate intertemporal constriction. Differs from *Agorophius pygmaeus* in derived features as follows: rostrum more dorsoventrally compressed; supraorbital process of maxilla not expanded far laterally; braincase more inflated at base of zygomatic process, with deep cleft between process and braincase; supraoccipital more hemispherical; and cheek teeth smaller, asymmetrical, and with diastemata.

Similar to Eurhinodelphinidae in having toothless premaxilla, elongate conical pterygoid hamulus, and thick postglenoid process. Similar to some extant Delphinidae in having well-developed interparietal and unfused mandibular symphysis. Similar to Waipatiidae and Squalodelphinidae in having pronounced cleft, presumably representing foramen spinosum, arising near foramen ovale and trending posterolaterally toward periotic along or near parieto-squamosal suture. Similar to some Delphinidae and Squalodontidae in having palate with scattered multiple small palatine foramina.

Presumed autapomorphies include thin spatulate edentulous rostral apex, formed by premaxillae, deflected ventrally, resulting in down-turned rostrum; relatively short rostrum; supraorbital process of maxilla not expanded laterally over supraorbital process of frontal; deep, narrow optic infundibulum; complex fine sutures between alisphenoid and squamosal; posterior maxillary cheek teeth occluding into facing diastemata between mandibular cheek teeth; and vestigial lower I1.

ETYMOLOGY.—After Clayton E. Ray, in recognition of his enduring and influential contributions to the study of fossil marine mammals.

TYPE LOCALITY.—Near intersection of North Yaquina Bay Road and Toledo Road, Lincoln County, Oregon, USA. Grid reference: SW 1/4, NE 1/4, Section 18, T 11S, R 10W on Toledo 15-minute quadrangle map (USGS) or about 44°37′06″N, 123°56′50″W. See Figure 1, and Snavely et al. (1976).

HORIZON.—Gray calcareous to brown leached massive mudstone of the Alsea Formation of Snavely et al. (1975). The specimen came from the most eastern exposure of Alsea Formation mapped by Snavely et al. (1975, 1976), near Toledo, Oregon.

TABLE 1.—Skull Measurements (in mm) of the standard skull measurements used by Perrin (1975), as well as measurements more appropriate for archaic odontocetes.

Condylobasal length, from tip of rostrum to posterior of occipital condyles	449+
Length of rostrum, from tip to line across posterior limits of antorbital notches (right and left notch, respectively)	235; 241
Width of rostrum at base, along line across posterior limits of antorbital notches	142
Width of rostrum at 60 mm anterior to line across posterior limits of antorbital notches	112
Width of rostrum at mid-length, at ~120 mm anterior to line across posterior limits of antorbital notches	75
Width of premaxillae at mid-length of rostrum	est. 61
Width of rostrum at 3/4 length, measured from posterior end	51+ (est. 57)
Distance from tip of rostrum to posterior of prenarial constriction	~198
Distance from tip of rostrum to anterior of bony naris	~203
Distance from tip of rostrum to most anterior portion of external wall of choana, immediately dorsal to pterygoid hamulus	340
Distance from tip of rostrum to broken tip of pterygoid hamulus	361
Preorbital width, at level of frontal-lacrimal suture	173
Supraorbital width, at middle of orbit	183
Postorbital width, across apices of postorbital processes	207
Depth from vertex to roof of orbit	41
Maximum width across narial aperture	31
Maximum width across zygomatic processes of squamosals	est. 238
(width from right process to midline)	119
Maximum width of premaxillae	89
Maximum width between posterolateral sulci	71
Distance from antorbital notch to apex of ascending process of right premaxilla	63
Distance from antorbital notch to apex of supraorbital process of right maxilla	80
Maximum distance between posterior apices of supraorbital processes of maxillae	125
Distance from midline of right internal ventral infraorbital foramen	36
Depth from vertex of right internal ventral infraorbital foramen	19
Median length of nasals on vertex	23+
Maximum length of right nasal on vertex	46
Distance anterior to antorbital notch of anterior border of nasals	~18
Median length of frontals on vertex	~81
Distance behind antorbital notch of anterior of frontals on vertex	86
Median length of parietals/interparietals on vertex	~39
Minimum parietal/interparietal width, at level of temporal lines	36
Parietal width, at dorsoventral midpoint of intertemporal region (35 mm ventral to vertex) and halfway along intertemporal region	82
Distance from posterior of occipital condyle to anterior apex of supraoccipital	99
Vertical external height of braincase, from midline of basioccipital to dorsal extremity of supraoccipital	107
Maximum length of right temporal fossa, point to point from most anterior portion of orbitotemporal crest on frontal to most posterior boundary of fossa	125
Minimum length of right temporal fossa, point to point from postorbital ridge on frontal to most anterior portion of base of zygomatic process	88
Maximum dorsoventral depth of right temporal fossa, from dorsal surface of intertemporal region to temporal angle	64
Maximum transverse width, from apex of right zygomatic process to braincase wall	55
Projection of premaxillae beyond maxillae, measured from tip of rostrum to line across anteriormost tips of maxillae in dorsal view	~24
Distance from posteriormost end of median suture between nasals to anteriormost apex of supraoccipital	139
Length of right orbit, from anterior apex of orbit to ventral apex of postorbital process	51
Median length of palatines	72
Maximum transverse width across palatines	91
Maximum length of left pterygoid	67+
Distance from tip of hamulus of left pterygoid to posteriormost portion of occipital condyle	78+
Maximum width of choanae	est. 48
Distance from most anterior portion of wall of left choana to most posterior portion of occipital condyle	105
Distance from hindmost portion of vomer to hindmost portion of occipital condyle	49
Width across paroccipital processes	est. 216
(width from right process to midline)	108
Distance from most anterior portion of right pterygoid sinus fossa to most posterior portion of occipital condyles	~143
Length of upper right tooth-row, from hindmost margin of most posterior alveolus to tip of rostrum	206
Distance from upper right canine to tip of rostrum	est. 61
Distance from position of posterior tooth to antorbital notch	59

TABLE 2.—Measurements of periotic. Not all the standard measurements suggested by Kasuya (1973) for odontocete periotics could be made. Measurements for the right periotic are to the nearest 0.5 mm.

Maximum anteroposterior length of exposed portion of periotic, from anterior apex of anterior process to level of posterior of pars cochlearis	37.0
Maximum anteroposterior length of pars cochlearis	23.0
Maximum transverse width of pars cochlearis, from internal edge to fenestra ovalis	~9.5
Maximum dorsoventral depth of anterior process	~16.5
Length of anterior process, from anterior apex of anterior process to level of anterior of pars cochlearis	14.0
Maximum transverse width of periotic, internal face of pars cochlearis to apex of lateral tuberosity	21.0
Maximum width of anterior process at base	13.0

AGE AND CORRELATION.—Upper Zemorrian Stage, late Oligocene. The Alsea Formation at the locality of USNM 256517 is faulted against the underlying upper Eocene Nestucca Formation, so that stratigraphic position of the specimen relative to the base of the Alsea Formation cannot be determined. Ellen J. Moore (USGS, pers comm., 1981) stated that foraminifera collected about 200 m south of the odontocete locality indicate an upper Zemorrian or late Oligocene age, and that molluscs collected about 300 m northwest of the odontocete locality indicate "Blakeley" Stage or late Oligocene. Domning et al. (1986) gave more details of the stratigraphy of vertebrate-bearing strata of this part of Oregon. Absolute ages for international units have been refined since 1986, so that the age for the Alsea Formation is presumably in the range of 30–23 Ma.

DESCRIPTION.—*General Features of Skull* (Figures 2–17; measurements in Tables 1–3): The skull is telescoped, with a plate-like supraorbital process of maxilla present dorsal to the supraorbital process of the frontal, the supraoccipital is thrust forward, and the short parietal is present in a distinct intertemporal constriction. Teeth are heterodont. Apart from the apex of the rostrum, there is little obvious postmortem distortion, and the asymmetry at the base of the rostrum appears to be real.

Cranium: The cranial portion of the skull, behind the antorbital notches, is long relative to the condylobasal length (Figure 2A). In lateral view (Figure 8A,C), the dorsal profile of the cranium is roughly straight, without an obvious raised vertex, and the dorsal and ventral profiles are more or less parallel. Viewed thus, the orbit clearly lies dorsal to the level of the lateral border of the rostral part of the maxilla (base of rostrum), the remnant of infraorbital process of maxilla, and the jugal. Presumably, the nasofacial (maxillo-naso-labialis) muscle originated from the maxilla both on the rostrum and dorsal to the orbit. In dorsal view (Figures 2A, 3), the posterior limit of the origin of nasofacial muscles is marked by the ridge that runs from the apex of each postorbital process smoothly medially and dorsally onto the fronto-parietal suture. Seen thus, the profile of the posterior of the face is anteriorly concave.

In dorsal view (Figures 2A, 3), the maxilla and frontal cover little of the temporal fossa, and the intertemporal constriction, formed by parietal and interparietal, is prominent. A long snout of nasal and frontal roofs the nares and olfactory cavity. A prominent orbitotemporal crest (temporal crest of Fordyce, 1994) delimits the dorsal edge of the fossa. Within the fossa, the lateral wall of the braincase is not particularly inflated except toward the base of the zygomatic process of the squamosal.

In lateral view (Figures 8A,C, 9), the external nares open more than 20 mm anterior to the level of the antorbital notch. The internal nares (choanae) open level with the apex of the supraoccipital and the middle of the pterygoid sinus fossa, indicating inclined rather than subvertical narial passages. Anteroposterior separation between internal and external nares also is emphasized by the long ventral exposure of the palatines (Figures 2D, 4).

Rostrum: The triangular rostrum is short, about as long as the cranium, and is broad at the base. The apex is blunt, with its apical 10 mm formed only by premaxillae (Figures 2A, 3, 5C) that are dorsoventrally thin and, individually, spatulate. Farther posteriorly, the rostral edges are straight until 20–35 mm anterior to the dorsoventrally deep antorbital notches. Here, at point of maximum width, the rostrum is asymmetrical, with the incomplete right side flared out laterally more than the complete left side. The antorbital notches, which appear wide and shallow in dorsal view, are asymmetrical, with the left notch more open than the right. In lateral view (Figures 8A,C, 9), the anterior half of the rostrum is thin, but rostral depth increases markedly toward the cranium as the premaxillae and maxillae become more elevated, and the rostrum is steep sided behind the external nares.

As viewed laterally (Figure 8A), the ventral profile of the rostrum is concave, with its tip depressed relative to the basicranial axis. A postmortem break distorts the tip dorsally, but the mandible (Figure 8B,D) indicates the original profile of the rostrum. In transverse profile, the maxillary part of the palate is flat to slightly convex (Figure 8E), but for a slightly concave region posterolaterally.

TABLE 3.—Measurements of mandible. Standard measurements of the right mandible, after Perrin (1975) are to the nearest 1 mm.

Tooth-row length, from posterior margin of most posterior alveolus to tip of mandible	221
Maximum length of mandible	334+ (est. 380)
Maximum height of mandible, perpendicular to maximum length	90 +

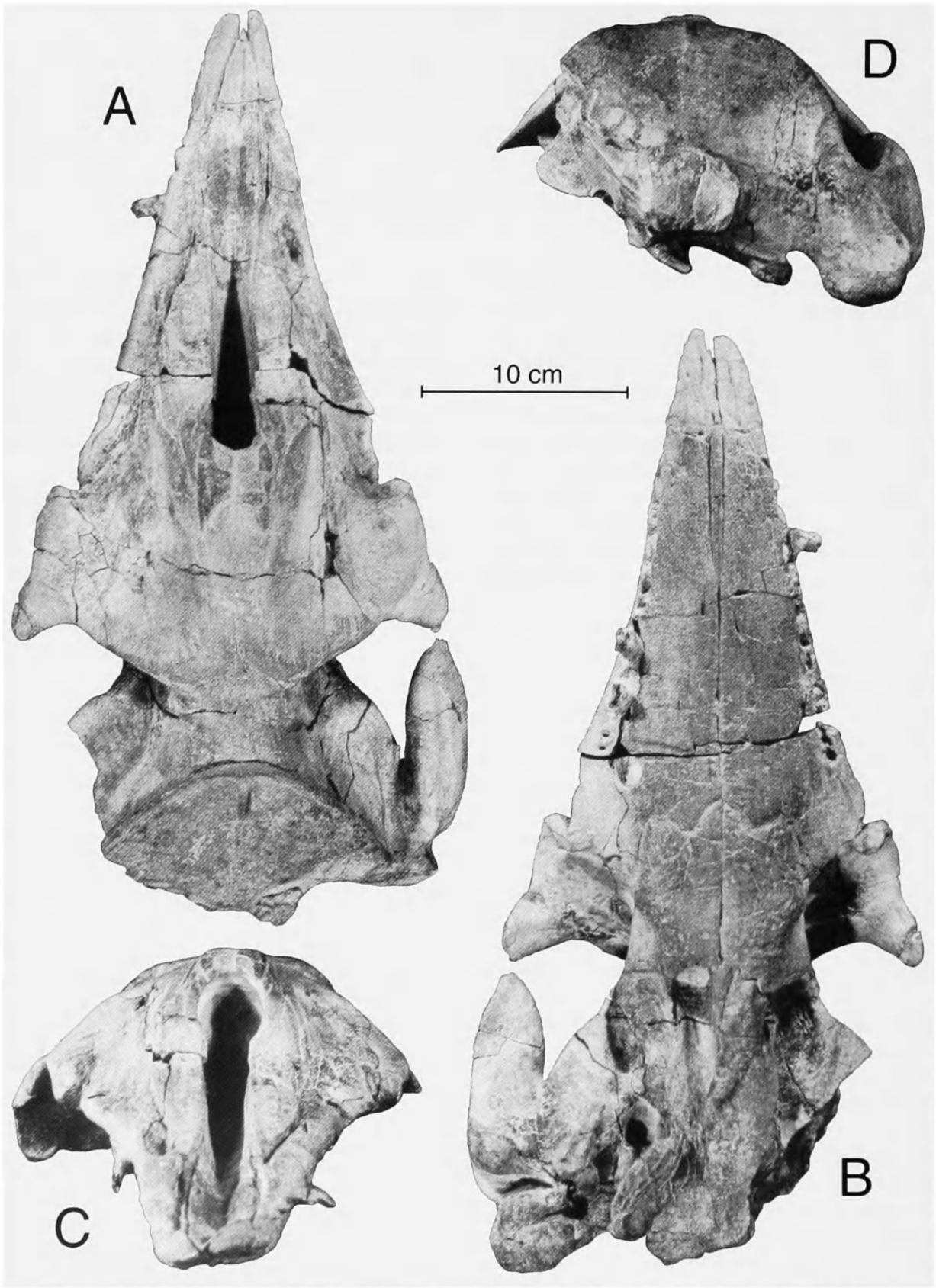

FIGURE 2.—*Simocetus rayi*, USNM 256517, holotype skull: A, dorsal; B, ventral; C, anterior; D, posterior. (Scale bar=10 cm.)

A prominent mesorostral groove dominates the rostrum anterior to the nasals. The groove is wide and shallow anteriorly, but it deepens and narrows behind the premaxillary foramina to become about as wide as deep at the mid-length of the rostrum. Farther posteriorly, the groove is narrow, deep, parallel-sided, and U-shaped, with a minimum width at an indistinct prenarial constriction about 35 mm in front of the nasals (Figures 2A, 3). (The prenarial constriction was inadvertently termed internarial

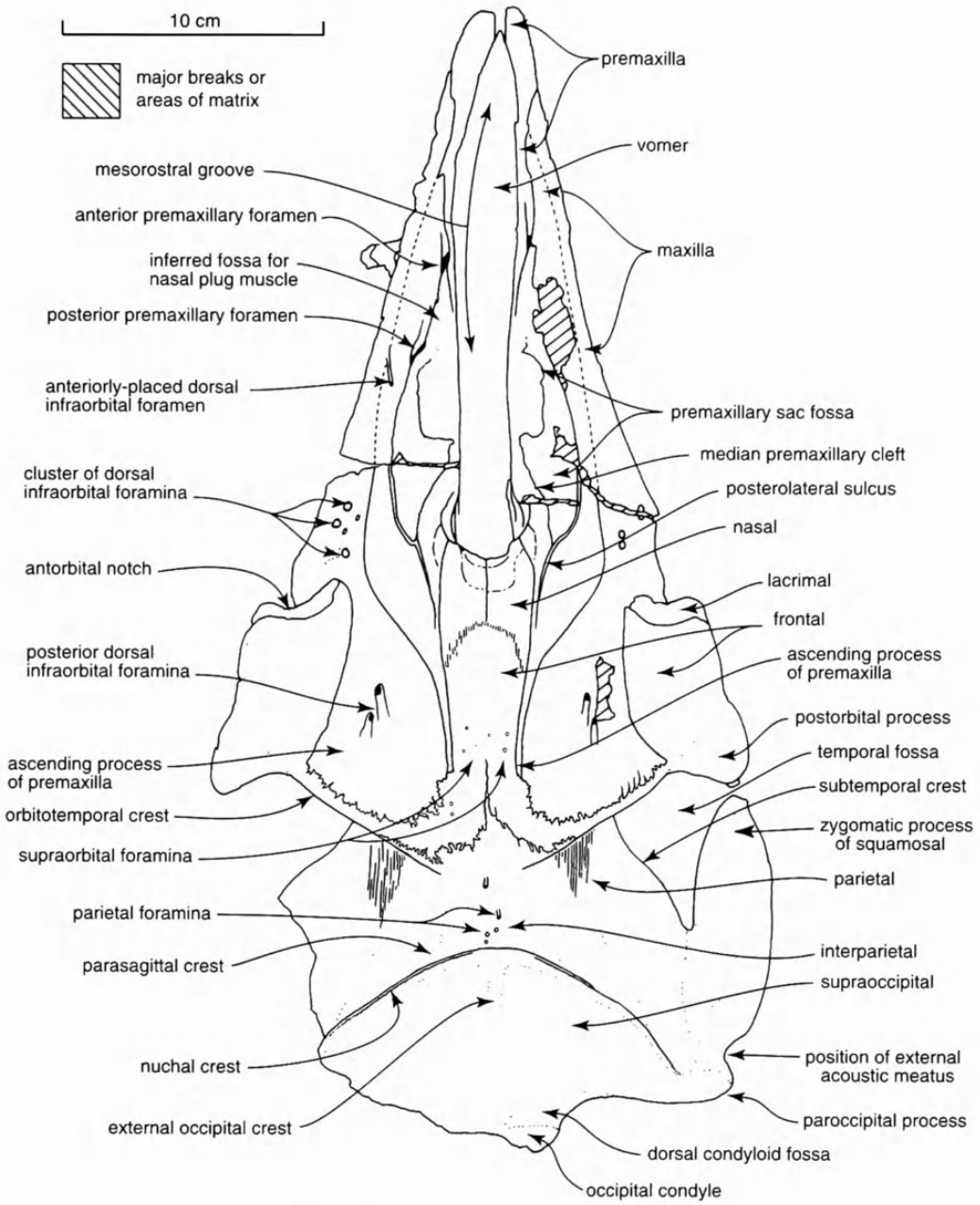

FIGURE 3.—*Simocetus rayi*, USNM 256517, dorsal view of holotype skull, based upon Figure 2A, showing main features. (Scale bar=10 cm.)

constriction by Fordyce (1994:149.)

Premaxilla: Three regions of the premaxilla command attention: the rostral apex, the premaxillary sac fossa, and the portion at and posterior to the nares. Most of the premaxilla lies on the rostrum, anterior to the antorbital notch. Anteriorly, the premaxillae lie close together for their apical 10 mm, separated by only a few millimeters at the open incisive suture (Figures 2A,B, 3, 4, 5C). Each premaxilla forms the thin spatulate anterior about 27 mm of the dorsal surface and margin of the rostrum. Apically, the well-preserved ventral (or palatal) surface of the premaxilla lacks alveoli and is interpreted as edentulous (Figure 5C). Ventrally, about 5 mm from the medial edge, each premaxilla carries a long, shallow, narrow groove that originates posteriorly at a feature presumed to be the palatine fissure. This fissure lies at the junction of premaxilla, maxilla, and vomer, about 58 mm posterior to the rostral apex. (Formerly, it was suggested that the palatine fissure is absent in Cetacea; Kellogg, 1936.) Anteriorly, the groove ends at a shallow depression presumed to be for the vomeronasal (Jacobson's) organ, about 8 mm behind the apex of the rostrum (Figure 5C).

Dorsally, the premaxillary sac fossa (premaxillary plate or spiracular plate of some authors), associated sulci, and foramina dominate the premaxilla. The premaxillary sac fossa is the long, elevated, and rather tabular dorsal surface of the premaxilla bounded by the posterolateral sulcus and the mesorostral groove (Figures 2C, 6). In living odontocetes, this surface carries a lobe of the nasal passages, the premaxillary sac (Mead, 1975). The fossa is narrow and pointed anteriorly. Its depressed lateral edge between 115 mm and 140 mm from the rostral apex perhaps marks the origin for the nasal plug muscle, al-

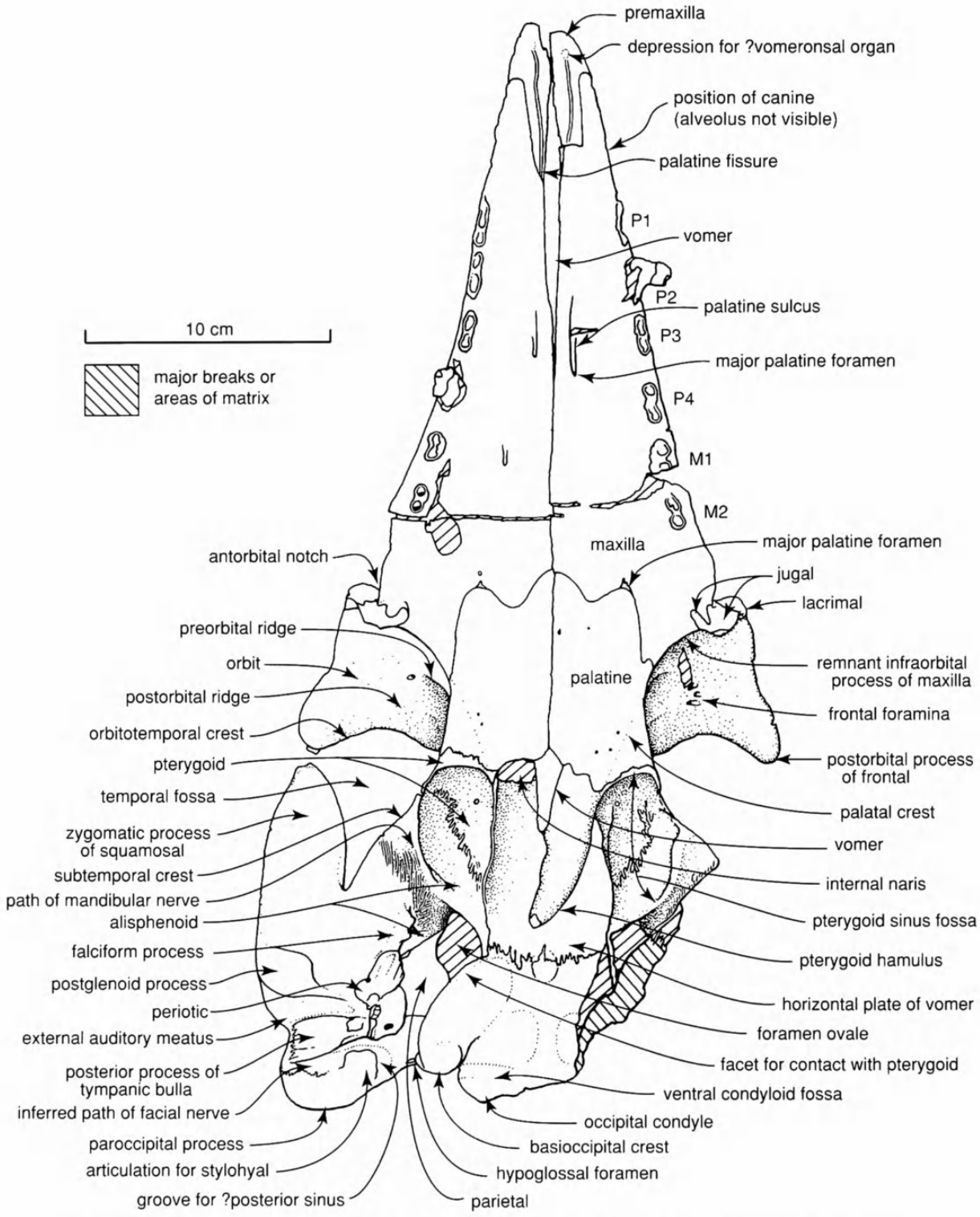

FIGURE 4.—*Simocetus rayi,* USNM 256517, ventral view of holotype skull, based upon Figure 2B, showing main features. (Scale bar=10 cm.)

though the bone here is smooth rather than rough. Farther posteriorly, the premaxillary sac fossa widens as its tabular dorsal surface rises above the level of the rest of the rostrum. The fossa reaches a width of about 25 mm level with the indistinct prenarial constriction, then narrows abruptly as the premaxilla rises toward the nasal.

Immediately lateral to the anterior part of the premaxillary sac fossa are two large premaxillary foramina, inferred to transmit branches of the internal maxillary artery and associated nerves. The anterior premaxillary foramen opens within the premaxilla (seen on the right, obscured on the left) into an anteromedial sulcus (sensu Barnes, 1978) on the dorsal surface, about 95 mm behind the apex of the rostrum and just lateral to the mesorostral groove. The posterior premaxillary foramen

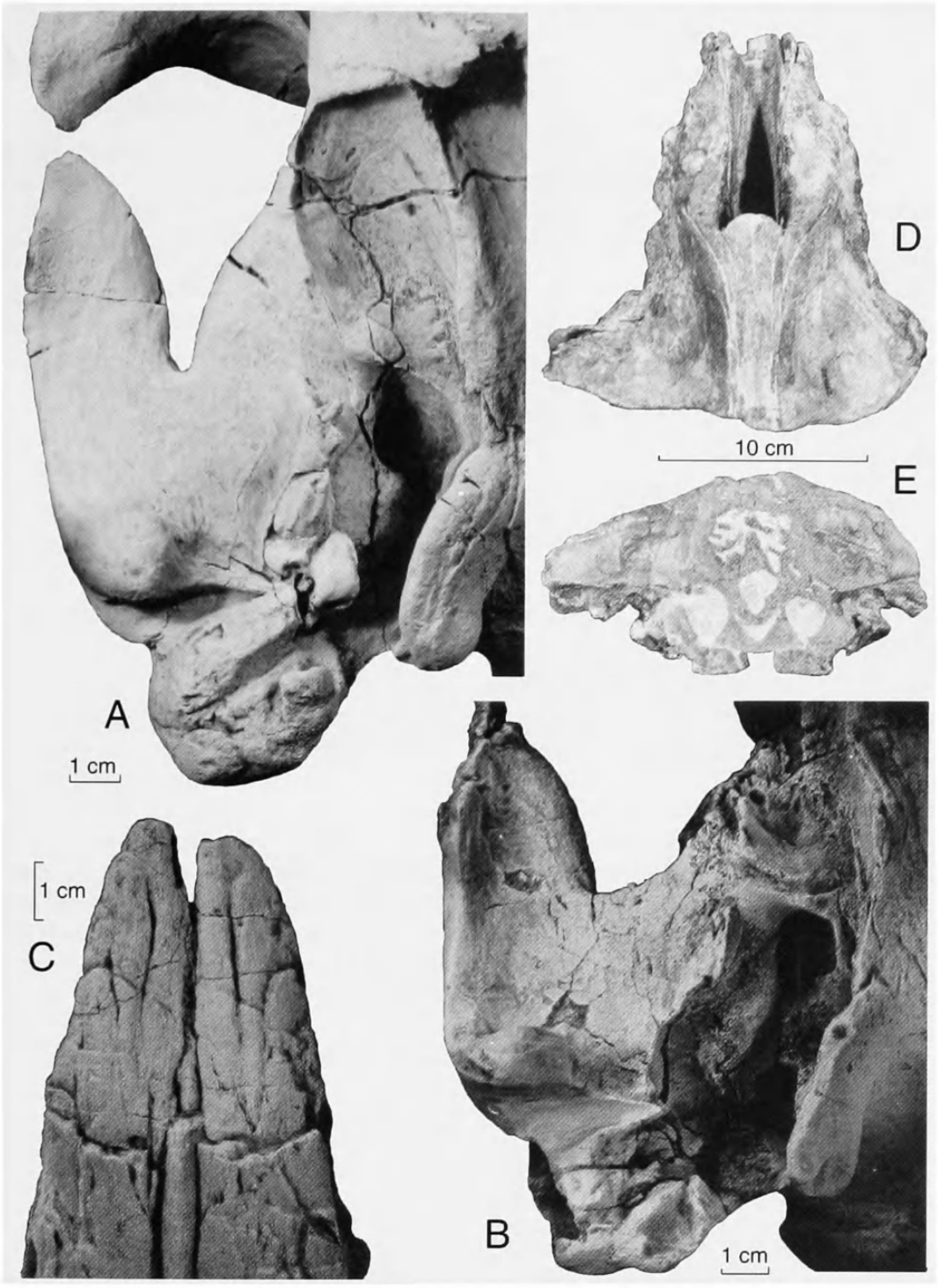

FIGURE 5.—*Simocetus rayi,* USNM 256517, and unnamed odontocetes USNM 205491 (Oligocene, Oregon) and USNM 299482 (Oligocene, Washington): A–C, whitened with ammonium chloride; A, holotype skull of *S. rayi,* USNM 256517, right basicranium; B, skull of unnamed odontocete USNM 205491 (Oligocene, Oregon), for comparison with *Simocetus rayi;* C, holotype skull of *S. rayi,* USNM 256517, detail of ventral surface of rostrum; D,E, incomplete skull of unnamed odontocete USNM 299482 (Oligocene, Oregon); D, dorsal view, showing elongate nasals over snout; E, posterior view of eroded section through olfactory cavity showing turbinals within olfactory cavity. (Scale bar=10 cm.)

(best preserved on the left) opens lateral and slightly ventral to the apex of the premaxillary sac fossa, 135–150 mm from the rostral apex (Figures 2A, 3). Posteriorly, the posterolateral sulcus deepens and narrows as it rises dorsomedially toward the nasals; it can be traced about 25 mm behind the level of the external nares. The posteromedian sulcus is possibly represented by an indistinct, wide, shallow groove that originates laterally near the apex of the fossa and trends posteromedially toward the elevated internal edge of the premaxilla.

Another fine sulcus, interpreted as the median premaxillary

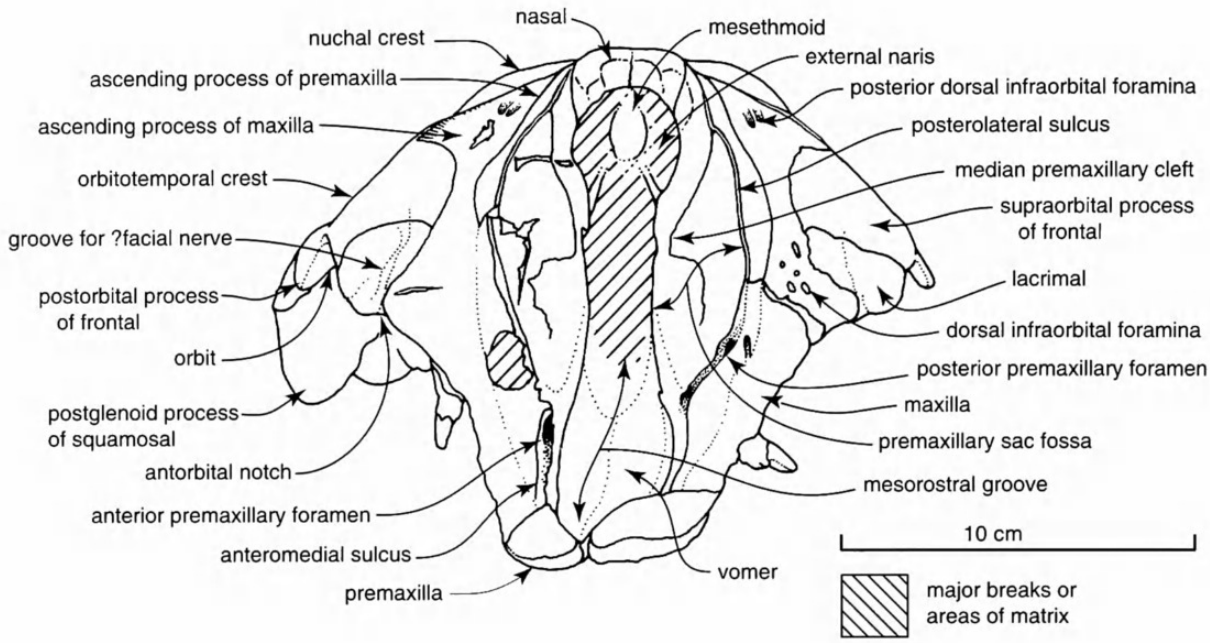

FIGURE 6.—*Simocetus rayi,* USNM 256517, anterior view of holotype skull, based upon Figure 2C, showing main features. (Scale bar=10 cm.)

cleft of Fordyce (1994:149), appears as a fissure in the otherwise smooth dorsal surface of the premaxillary sac fossa. In *S. rayi,* the anterior origin of the median premaxillary cleft is obscure, but in USNM 299482 (an undescribed archaic odontocete; Figure 5D), the median premaxillary cleft appears to originate at the posterior premaxillary foramen. It meanders posteriorly then diverges abruptly toward the internal edge of the premaxillary sac fossa at about the mid-length of the fossa; thence it trends farther posteriorly and slightly externally to contact the posterolateral sulcus at about the level of the anterior end of the nasal. Broken sections through the median premaxillary cleft in USNM 299482 indicate that it extends far ventrally within the premaxilla, and the same is inferred for *S. rayi*. The function of this sulcus is uncertain.

Lateral to the premaxillary sac fossa and the posterolateral sulcus are remnants of a thin, elongate flange of premaxilla

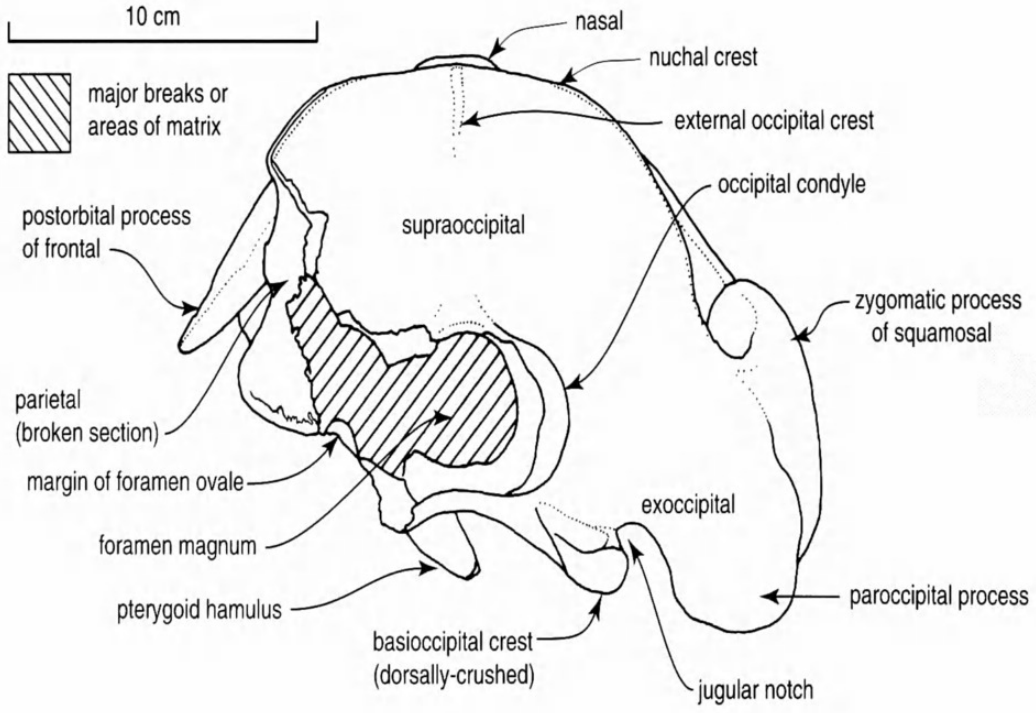

FIGURE 7.—*Simocetus rayi,* USNM 256517, posterior view of holotype skull, based upon Figure 2D, showing main features. (Scale bar=10 cm.)

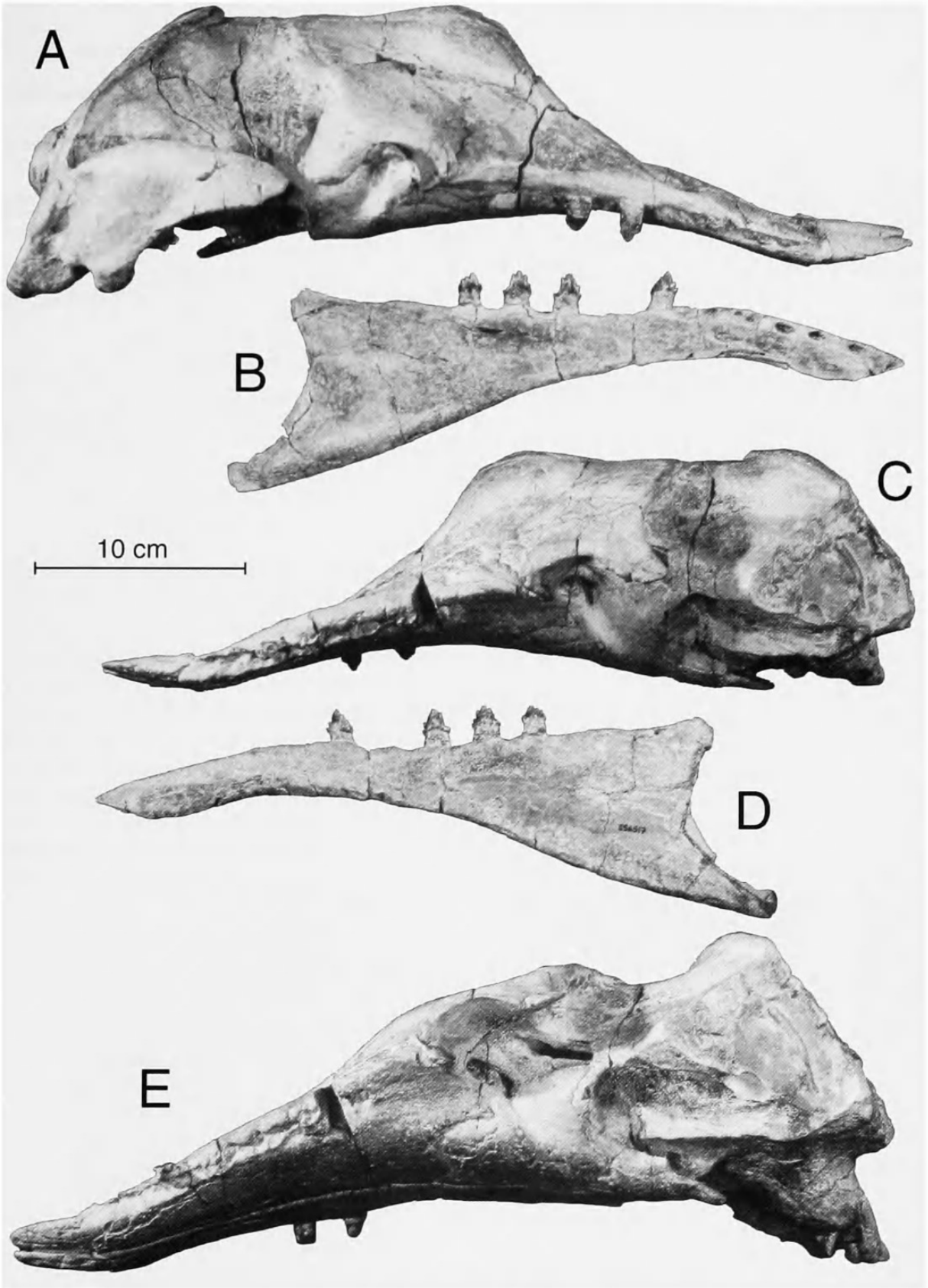

FIGURE 8.—*Simocetus rayi,* USNM 256517, holotype skull and right mandible: A, skull, right lateral; B, right mandible, lateral (buccal) view; C, skull, left lateral view; D, right mandible, medial (lingual) view; E, skull, oblique ventrolateral view, left side. (Scale bar=10 cm.)

that, before being eroded, originally overlay the dorsal surface of the maxilla (Figure 2A,C). Posteriorly, at the level of the nasal, this thin portion of premaxilla becomes the posterolateral plate; the plate is conspicuous in lateral view (e.g., Figure 9). Dorsally, the posterolateral plate passes into the posteromedial process. The left and right posteromedial processes are sym-

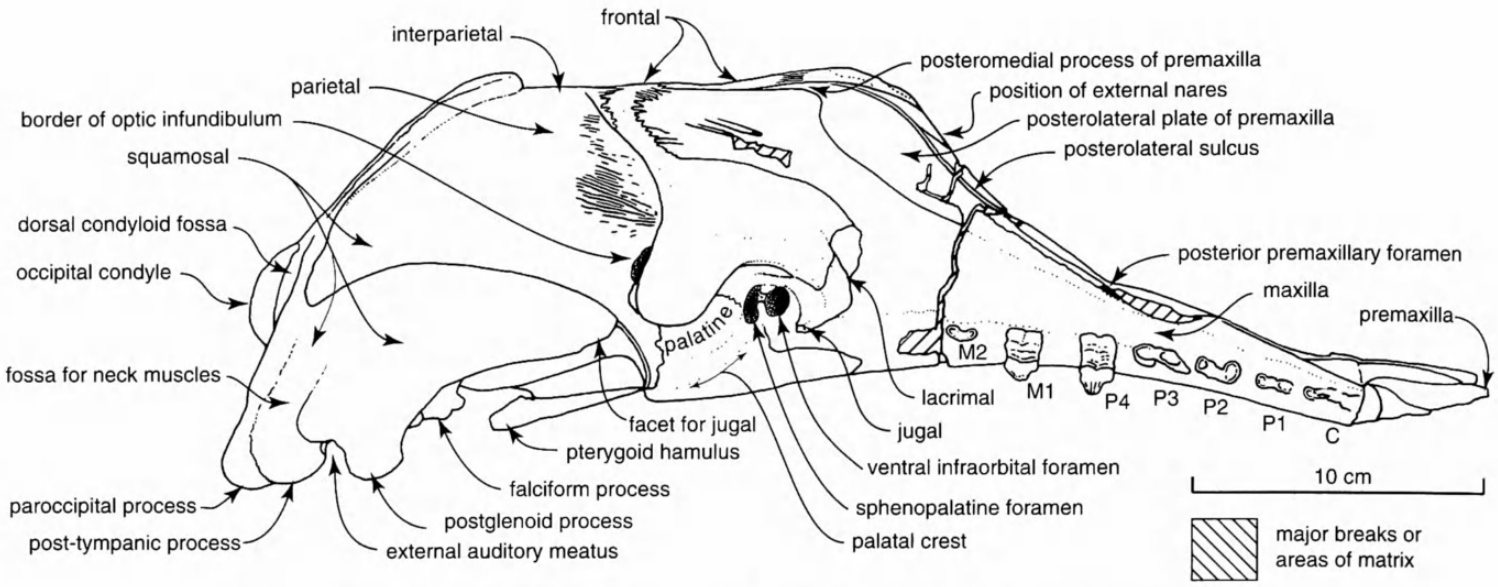

FIGURE 9.—*Simocetus rayi,* USNM 256517, right lateral view of holotype skull, based upon Figure 8A, showing main features. (Scale bar=10 cm.)

metrical; each is narrow (<2 mm wide), parallel sided, and long, extending far posteriorly between the maxilla and the nasal-frontal. The right process reaches about 95 mm behind the nares, well posterior to the naso-frontal suture and the orbit (Figures 2A, 3, 9).

Maxilla: Ventrally, the maxilla forms most of the rostrum, including the massive thick dorsoventrally rounded lateral edge, which extends to within about 25 mm of the rostral apex. Anterior teeth lie at the edge of the maxilla, but the posterior teeth lie a little medially (Figures 2B, 4). There are alveoli for a canine (matrix-filled with eroded borders, on the rostral margin of the maxilla and not readily seen in figures) and six cheek teeth, identified as P1–4 and M1–2; teeth are detailed below. Anteriorly, the alveoli on the rostral margin are too eroded to be sure of orientations and fine structure, but posterior alveoli are separated by diastemata (interdental spaces) long enough to accommodate crowns of lower cheek teeth. An indistinct embrasure pit lies between and slightly medial to right P4 and M1 (Figure 2B). M2 lies about 35 mm anterior to the antorbital notch (Figures 2B, 4). There are no obvious alveolar juga, and the alveolar process is not distinct from the rest of the maxilla.

Most of the rostral (oral, ventral) surface (palatine process) of the maxilla is gently convex in transverse profile, but, posterolaterally near the antorbital notch, the surface is concave

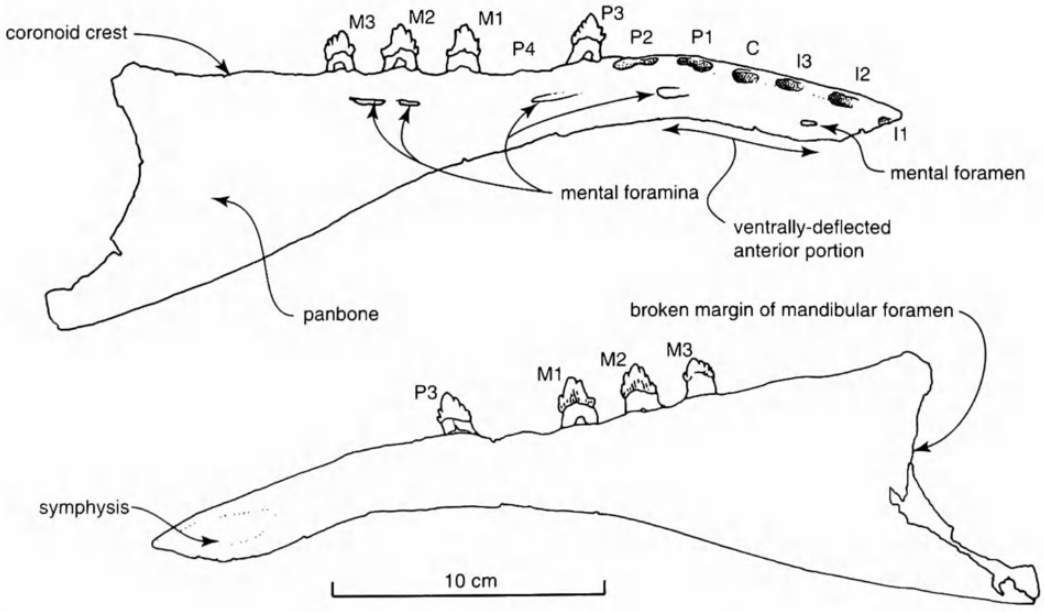

FIGURE 10.—*Simocetus rayi,* USNM 256517, right mandible, showing main features: A, lateral (buccal), based upon Figure 8A; B, medial (lingual), based upon Figure 8C. (Scale bar=10 cm.)

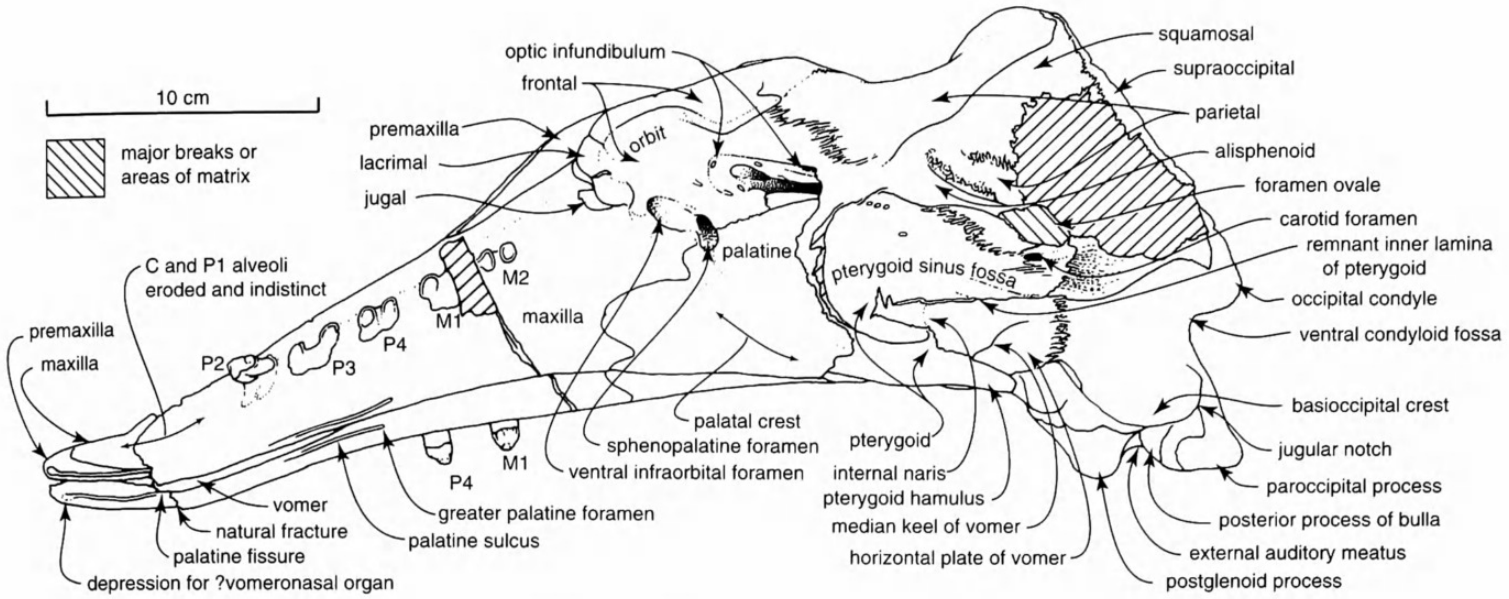

FIGURE 11.—*Simocetus rayi,* USNM 256517, oblique ventrolateral view of holotype skull, based upon Figure 8E, showing main features. (Scale bar=10 cm.)

(Figures 2B, 8E). Nearby, the conspicuous and simple maxillary-palatine suture (Figure 2B) traces an S-shaped profile as it runs laterally from the midline. A short and narrow major (or greater) palatine sulcus at the maxillary-palatine suture (Figure 4) indicates a major palatine foramen. Farther anteriorly, another aperture of the major palatine foramen opens into a palatine sulcus medially, about level with P3 and P4. Smaller foramina that open ventrally on the maxilla probably represent other multiple openings for the palatine foramina.

Posteriorly, the maxilla has only a small orbital surface. Here, a prominent transverse ridge of the maxilla in the orbital wall, immediately below the ventral infraorbital foramen (orbital opening of infraorbital canal, or maxillary foramen of authors) is a vestigial infraorbital process. Because the ridge is not prolonged posteriorly, there is neither a maxillary tuberosity nor a pterygopalatine fossa. Medially, a stout projection of the maxilla partly separates the ventral infraorbital foramen from the sphenopalatine foramen (Figures 11, 12).

The ventral infraorbital and sphenopalatine foramina open within a common infundibulum anterior to the preorbital ridge (Figures 8E, 11–13) and topographically within the orbit. Within the infundibulum, the larger infraorbital portion lies

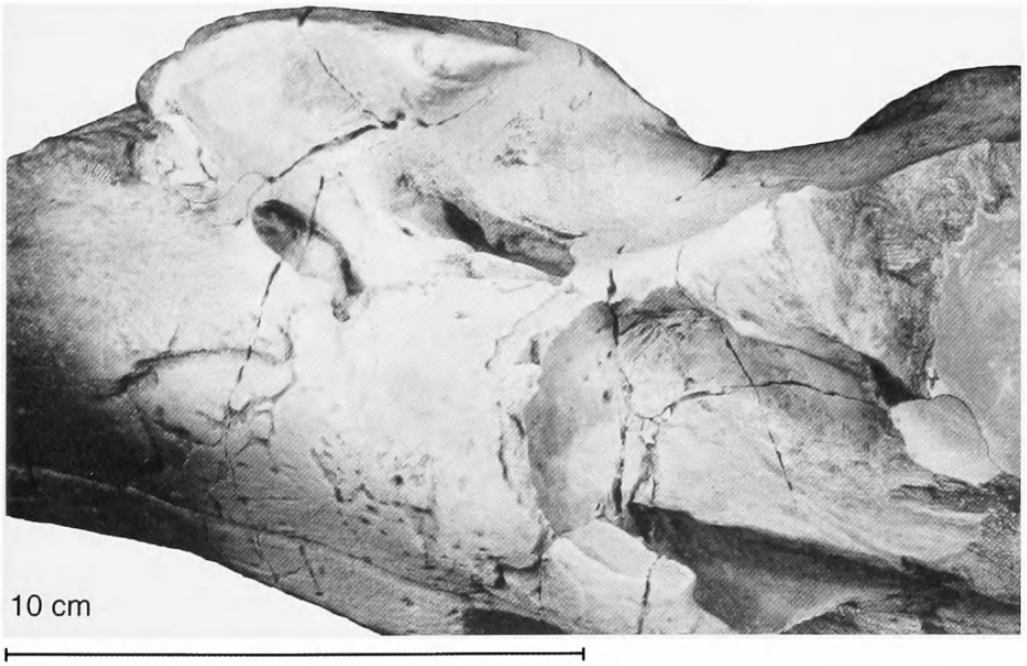

FIGURE 12.—*Simocetus rayi,* USNM 256517, oblique ventrolateral view of left orbit of holotype skull. Skull whitened with ammonium chloride. (Scale bar=10 cm.)

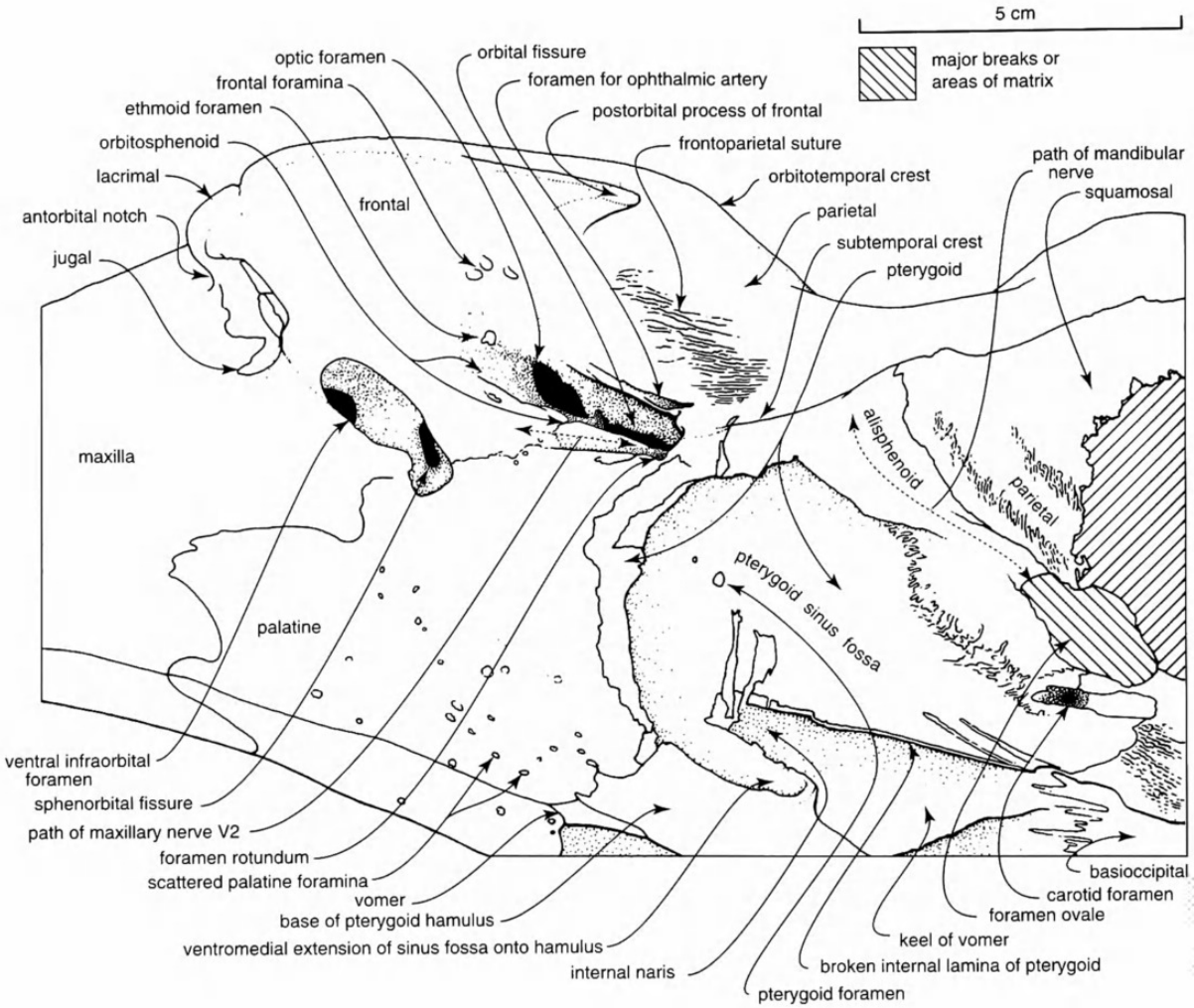

FIGURE 13.—*Simocetus rayi*, USNM 256517, oblique ventrolateral view of left orbit of holotype skull, based upon Figure 12, showing main features. (Scale bar=5 cm.)

medially in the anterior wall of the orbit, whereas the smaller sphenopalatine portion lies posteroventrally on the lateral wall of the skull below the orbit. The infundibulum is bounded ventrally by the maxilla, dorsally and anterolaterally by the frontal, and posteriorly and posteroventrally by the palatine; it is uncertain if the lacrimal contributes to the lateral border. Anteriorly, the large ventral infraorbital foramen gives rise to the infraorbital canal from which the dorsal infraorbital foramina (maxillary foramina of authors) and premaxillary foramen open on the dorsal surface of the skull. The small sphenopalatine foramen lies posteriorly in the roof of the infundibulum, where it is directed dorsomedially.

As seen ventrally, the maxilla at the antorbital notch is invaded by two small lobes of the jugal (zygomatic bone), a shorter lateral lobe and a longer medial lobe. That part of the maxilla bounded by the two lobes of the jugal may represent the zygomatic process of the maxilla, although the zygomatic process in other mammals usually lies laterally on the skull wall. There is no clear evidence in the maxilla here of an anterior lacrimal crest, lacrimal notch, lacrimal sulcus, or lacrimal canal.

Dorsally on the rostrum, the maxilla is rounded in transverse profile until about the level of the posterior premaxillary foramen, behind which its surface becomes slightly concave. Dorsal infraorbital foramina open on the maxilla; on the left, the anteriormost foramen opens near the posterior premaxillary foramen (150 mm behind the rostral apex), and a prominent cluster of foramina lies farther posteriorly near the antorbital notch. Because of poor surface detail on the right side, it is not clear whether the number and size of foramina is symmetrical from left to right, although the two maxillae clearly are asymmetrical in profile. These large, multiple, dorsal infraorbital foramina are taken to indicate that parts of the nasofacial muscles originated on the rostrum anterior to the antorbital notch.

The lacrimal bisects the maxilla at the antorbital notch, separating the rostral from the more-posteromedial facial parts of the maxilla (Figures 2C, 6). At the base of the supraorbital process, the maxilla does not expand laterally over the lacrimal; thus, it lacks an antorbital process.

Posterior to the lacrimal, the maxilla forms a long, roughly parallel-sided supraorbital process (ascending process, frontal process) that extends across the frontal and rises medially toward the vertex (Figures 2A, 3). Here, the maxillary surface is slightly concave from side to side, forming an indistinct facial fossa for nasofrontal muscles. Seen dorsally, the supraorbital process has a lateral margin that is gently concave rather than convex. Further, the supraorbital process is not expanded outward over the frontal. Because the left and right supraorbital processes are symmetrical, and there is no evidence of erosion or abnormal bone surface on maxilla and frontal, the lack of lateral expansion is taken as an original condition. Two posterior dorsal infraorbital foramina open posterodorsally in the supraorbital process of each maxilla; they lie about level with the mid-orbit as viewed laterally, about 15 mm below the level of the vertex, and about 40 mm lateral to the cranial midline. Each foramen opens posteriorly into a shallow widening groove; the anterior foramen is the larger. These foramina are taken to indicate that the maxilla here formed an origin for a significant volume of facial muscles. Nearby, the posterolateral corner of the supraorbital process is sharp, whereas the posteromedial corner is rounded. Posteriorly, the supraorbital process does not reach the level of the orbitotemporal crest of the frontal. By analogy with an undescribed archaic odontocete, USNM 299482 (Figure 5D), the straight and slightly raised medial border of the supraorbital process of maxilla probably overlies part of the posteromedial process of the premaxilla. Preservation is too poor to tell if the maxilla has a nasal crest within the bony naris.

Vomer: The vomer lines the prominent mesorostral groove where, in dorsal view, it reaches to within about 10 mm of the rostral apex (Figures 2A, 3). The vomer, and thus the mesorostral groove, is widest (about 28 mm) about 70 mm behind the rostral apex. Ventrally, the vomer is exposed as a short thin sliver (up to 7 mm wide) anteriorly on the palate, wedged between the premaxillae anteriorly and the maxillae posteriorly. A cross section of rostrum seen during preparation indicates that each side of the vomer widens to more than 25 mm within the rostrum. Farther posteriorly, a diamond-shaped medial exposure of vomer lies between the palatines and pterygoids (Figures 2B, 4); compared with most odontocetes, this exposure of vomer is quite large. Posterodorsally, this diamond-shaped exposure rises into a long median keel of vomer, which separates the choanae back to about the level of the foramen ovale (Figures 8E, 11–13). The slightly outward-flared horizontal plate of vomer, which roofs the choanae, extends back about 20 mm farther, about level with the anterior of the basioccipital crests. Presumably, the horizontal plate of vomer originally contacted the now-missing internal lamina of the pterygoid here.

Palatine: The broadly exposed palatine forms much of the posterior flat ventral surface (horizontal lamina) of the palate, and it is inferred to contribute to the hard palate as seen in other mammals but in contrast to living odontocetes. The prominent median interpalatine suture is about 71 mm long, and each palatine is more than 84 mm long, so that the pterygoid is separated widely from the maxilla. Anteriorly, the palatine extends well forward of the antorbital notch, whereas posteriorly the palatine reaches behind the level of the postorbital process of the frontal. Ventral and lateral faces of the palatine are separated by a gently rounded palatal crest that arises at the infundibulum for the infraorbital and sphenopalatine foramina and descends posteroventrally toward the pterygoid. There is no obvious pterygopalatine fossa. Above this palatal crest, the palatine carries a smoothly rounded surface posterior to the infraorbital infundibulum and ventral to the optic infundibulum; this surface is presumed to be the origin of the internal pterygoid muscle. Dorsally, there is no sphenopalatine notch, so that the orbital process and spheno-ethmoid lamina are continuous; sutures with frontal and orbitosphenoid are prominent. Posterodorsally, a few millimeters of the palatine contacts the parietal. Posteriorly, the suture with the pterygoid is conspicuous, without a lateral lamina of palatine, and the pterygoid sinus does not invade the palatine. Ventral sutures with the pterygoid and vomer are deep.

Grooves at the anterolateral corner of the maxillo-palatine suture form the major palatine sulcus and associated (matrix-filled) major palatine foramen, and small foramina scattered on the horizontal lamina represent minor palatine foramina. The palatine carries other scattered small foramina, some localized on the palatal crest.

At its anterodorsal limit, and within the orbit, the palatine contributes to a large common infundibulum for the more posteriorly placed sphenopalatine foramen and anteriorly placed ventral infraorbital foramen. The caudal palatine foramen (proximal opening of canal for palatine vessels and nerves) probably also opens here, although it is not visible.

Nasal: The small, dorsally convex, and anteriorly deflected nasals form the vertex of the skull at the prominent "snout," where they lie well forward of the orbits. In dorsal view, each nasal is sculptured anteromedially and is longer than it is wide. The gently convex lateral border is markedly longer than the medial border, which is marked by a slightly depressed internasal suture. The nasals are slightly asymmetrical in shape and sculpture, but it is uncertain if this is original or postmortem. Anteriorly, each nasal forms a thin downturned roof over the bony nares. The two nasals are separated posteriorly by the blunt narial process of the frontals, and the naso-frontal suture is slightly depressed.

Mesethmoid: The mesethmoid occurs in the posterior of the mesorostral groove (Figure 6), where it is some 32 mm high and 10–12 mm wide. Matrix obscures details. Presumably, the mesethmoid (mesorostral or septal) cartilage originally filled the mesorostral groove anterior to the ossified mesethmoid. A round element seen in cross section in the narial cavity above the large exposure of the mesethmoid could be a dorsal part of the mesethmoid; it is about 14 mm high and 9–10 mm wide. The ectethmoid is not apparent.

Frontal: On the vertex, the frontals form a long, narrow (~28 mm wide), median exposure posterior to the nasals and medial to the ascending processes of the premaxillae. Anteriorly, the frontals are fused to form a broad, bluntly rounded narial process, which partly separates the nasals. Posteriorly, a median interfrontal suture arises from the fronto-parietal suture to separate the frontals for about 30 mm. The frontals at the vertex carry at least 12 small ($\leq$1 mm diameter) scattered foramina, interpreted as remnant supraorbital foramina comparable with those of some Dorudontinae and archaic Mysticeti.

From the posterior limit on the vertex, a narrow continuous strip of frontal descends laterally toward the orbit, bounded by the supraorbital process of the maxilla (anterior) and parietal (posterior). The parietal margin has a well-developed foliate fronto-parietal suture, on which the orbitotemporal crest originates. In a dorsal or anterodorsal view (Figures 2C, 6) of the skull, the two orbitotemporal crests form a conspicuous semicircular posterior border of the face; the crests probably indicate the posterior limit of the origin of the nasofacial muscles. Each orbitotemporal crest grades laterally onto the supraorbital region, where it forms a strong ridge at the base of the postorbital process. The postorbital process is a wide, thin plate that descends steeply toward the apex of the zygomatic process of the squamosal; it does not extend far posteriorly. Farther anteriorly is the thick and robust orbital (supraorbital) part of the frontal, which is overlapped medially by the rather narrow ascending or supraorbital process of the maxilla. The preorbital process of the frontal appears blunt in dorsal view and is dorsoventrally thick, but it is the lacrimal that here forms the anterolateral part of the cranium at the antorbital notch.

As seen laterally, the orbit is strongly arched dorsally, contrasting with the shallow, long orbit in most odontocetes. Furthermore, its anterior profile is strongly concave posteriorly. The orbit lies above the level of the lateral border of the rostral part of the maxilla (above the base of the rostrum), but a little below the dorsoventral midpoint of the skull. The frontal forms most of the orbit, with some contribution of the lacrimal, jugal, and maxilla to the anterior wall. At least two presumed frontal foramina open in the roof of the left orbit about 30 mm internal to the edge of the orbit, just anterior to the postorbital ridge. Medially, the orbit passes into the deep groove of the optic infundibulum, where the narrow, slit-like ethmoid foramen (see left side; Figures 12, 13) for the ethmoidal vessel and nerve opens immediately anterior to orbitosphenoid-frontal suture. Other details of the optic infundibulum are given under the orbitosphenoid.

Posteriorly, the orbit is bounded by a strong postorbital ridge (crista orbitalis superior; Figures 2B, 4), which is indistinct laterally on the postorbital process but which becomes more distinct medially as it grades into the dorsal edge of the optic infundibulum (sensu Fraser and Purves, 1960). This ridge marks the anteroventral limit of origin of the temporalis on the frontal. The preorbital ridge (ventral orbital crest, crista orbitalis inferior), which normally delimits the anteroventral part of the orbit in mammals (Davis, 1964; Evans, 1993), is not developed laterally, but it is thick and low medially where it separates the optic infundibulum from the infraorbital infundibulum. There is no obvious pterygopalatine fossa.

Anteroventrally, the orbit is delimited by a strong ridge of jugal and maxilla at the posterior limit of the rostrum, to which the frontal does not contribute. Laterally, this ridge involves only the jugal (the lacrimal lies more dorsally), whereas farther posteromedially, the maxilla forms the ridge just ventral to the infundibulum for the infraorbital and sphenopalatine foramina. This ridge is a vestigial equivalent of the infraorbital process of the maxilla of other mammals.

Lacrimal: The lacrimal is unexpectedly prominent, and the facial surface is exposed well to dorsal view and not covered by the maxilla. It is transversely elongate and dorsoventrally thick in the anterior wall of the orbit but does not contribute to the roof of the anterior part of the orbit (posterodorsal limits of the lacrimal within the orbit are not clear). Medially, the lacrimal extends beyond the antorbital notch onto the rostrum; the left side is well preserved. There is no evidence of a fossa for the lacrimal sac, fossa for oblique muscle, or lacrimal canal, and an orbital crest cannot be identified.

Jugal: The jugal (zygomatic bone) is identified provisionally by analogy with the situation in young specimens of extant Ziphiidae, the only group of extant Odontoceti in which limits of the normally fused jugal and lacrimal can be determined easily. As seen ventrally, the left jugal in *S. rayi* has two anteriorly directed processes that invade the maxilla; the medial process is the larger. (Limits to the right jugal are obscure.) In the absence of a clear suture between the jugal and the more dorsal lacrimal, these two bones are presumed to be fused fully. Originally, a thin process of the jugal presumably underlay the orbit, passing posteriorly to contact the apex of the zygomatic process of the squamosal.

Parietal and Interparietal: The prominent, short, and transversely rounded intertemporal region is formed by the parietals and interparietal. The interparietal has a narrow medial exposure, is bounded by ill-defined serrate to foliate sutures with the parietal, and fully separates the parietals; it extends from the supraoccipital to the frontal. There is a low, indistinct median ridge but no sagittal crest. Anteriorly directed parietal foramina open on the interparietal.

Immediately lateral to the interparietal, each parietal is smooth with two indistinct subparallel parasagittal temporal crests (temporal lines, supratemporal crests of Novacek, 1986) developed posterolaterally (Figures 2A, 3). Anteriorly, about 17 mm from the midline, each parietal gives rise to a sharp orbitotemporal crest that passes laterally and slightly anteriorly onto the frontal. Here, at its frontal border, the parietal dorsally buttresses the supraorbital process of the frontal (Figure 2A). Farther ventrally, where, on the left, a prominent serrate suture is present (Figures 12, 13), the parietal extends a little anteriorly along the cranial wall. Anteroventrally, the parietal forms the posterior margin of the optic infundibulum, thus contributing to

the postorbital ridge, and it also contacts the palatine and pterygoid immediately ventral to the optic infundibulum (Figures 12, 13). Farther posteriorly, the parietal extends ventrally to the infratemporal crest (=subtemporal crest; Fordyce, 1994), but details of contact here with the alisphenoid are uncertain. Also within the temporal fossa, the posterior suture with the squamosal at the squamous border cannot be localized; on the broken left side, the parieto-squamosal suture is not identifiable on the preserved part of the braincase wall. The suture with the supraoccipital cannot be localized at the nuchal crest. Ventrally and posteroventrally, within the temporal fossa, the braincase widens markedly.

The parietal appears to be present in the basicranium dorsal and medial to the periotic. This identification is not certain because the in situ periotic covers the area where the parieto-squamosal suture is expected, and it is possible that the element here may be squamosal only. The parietal is, however, known to be present in the identical position in an archaic odontocete USNM 205491 (Figure 5B), which is comparable in basicranial grade to *S. rayi*. The parietal also occurs in this position in *Waipatia maerewhenua* Fordyce (holotype, OU 22095; see Fordyce, 1994, for discussion) and in a wide range of other odontocetes. Identified thus, the parietal forms the lateral border to the posterior lacerate foramen. Although the parietal extends medially toward the basioccipital, it does not contact the latter; thus the posterior lacerate foramen and more anteriorly placed foramen ovale are confluent, with a constricted apostrophe-like profile. The posterior suture of the parietal with the exoccipital can be localized only to within a few millimeters. Anteromedially, this basicranial part of the parietal forms a wedge that extends forward, bounded laterally by the alisphenoid, to form part of the foramen ovale.

Supraoccipital: The broad supraoccipital slopes forward at about 45° from horizontal. It is roughly hemispherical in dorsal or posterior view (Figures 2A,D, 3, 7), whereas in lateral view the longitudinal profile is convex, more so laterally than medially. Anterodorsally, the surface of the supraoccipital is raised, but there is no distinct projecting external occipital protuberance. Also anterodorsally, a short low external occipital crest lies just to the right of the midline (Figure 7), but there is no significant asymmetry. Below the external occipital crest is a faint median depression that passes ventrally into a raised region, without nuchal tubercles, just above the foramen magnum. The anterolateral quadrants of the supraoccipital are gently convex dorsally.

The apex of the supraoccipital at the nuchal crest rises dorsally about 6 mm above the adjacent interparietal and parietals. Laterally, the nuchal crest (here sometimes termed the lambdoidal crest) overhangs the parietal and squamosal by up to 10 mm. The crest descends steeply toward the exoccipital and, at the posterior of the temporal fossa, swings abruptly forward onto the zygomatic process of the squamosal (forming the temporal crest of some authors).

Exoccipital: Dorsally, the exoccipital is fused completely with the supraoccipital, so that the limits of these elements are uncertain. The right condyle lacks the medial border, so that its outline is incomplete; as preserved it is reniform and transversely narrow in posterior view. Enough remains to show that, originally, the condyles formed an articular surface with a primitively wide and oblate (rather than subcircular) profile (Figures 2D, 7), with a circular foramen magnum. The dorsal intercondylar notch is broad and shallow, although remnants indicate a more narrow ventral notch. The condyle lacks an elevated pedicle, but the dorsal condyloid fossa is prominent and deep. The ventral condyloid fossa is open and spacious but less clearly delimited. Preservation is too poor to judge the state of the condyloid foramen (in other mammals, for condyloid vein between basilar sinus and sigmoid sinus), but presumably the foramen is small or absent as in other odontocetes.

The long axis of the rather tabular and roughly parallel-sided paroccipital process extends ventrolaterally and posteriorly (Figures 2D, 6, 14B, 16) to almost reach the level of the outer face of the zygomatic process of the squamosal. Ventrally, the apex reaches below the level of the basioccipital crest (although the latter is pushed dorsally by postmortem crushing) and, viewed dorsally, extends posteriorly almost to the level of the posterior of the condyle.

In lateral view, the paroccipital process appears mostly thin, but distally, at its contact with the post-tympanic process of the squamosal, it thickens markedly. This thick apex, seen ventrally, is nodular, wider than it is long, and roughly oval in profile. The diffuse articulation for the stylohyal lies ventral to a horizontal, anteriorly facing, narrow groove or notch interpreted as the fossa for a posterior sinus, which originated from the elliptical foramen of the bulla. Immediately dorsally, between the exoccipital and posterior process of the tympanic bulla, is an open groove that probably carried the facial nerve externally; it is not clear whether the paroccipital process contacts the posterior process of the bulla in the roof of this groove, or whether 1–2 mm of squamosal lies between these elements. Farther dorsomedially, the anterior face of the paroccipital process is convex, without any excavated fossa, but the open region between the paroccipital process and the pars cochlearis of the periotic probably held a lobe of the peribullary sinus. This interpretation, based upon study of extant odontocetes, differs from that of previous authors (e.g., Fraser and Purves, 1960), who have identified this open region in diverse odontocetes as the fossa for the posterior sinus. Farther medially, the exoccipital bounds all of the jugular notch and descends onto the base of the basioccipital crest. The notch is wide and shallow, and the small hypoglossal foramen (for nerve XII and perhaps the vein of the hypoglossal canal) opens anteromedially. Immediately anterodorsal to the hypoglossal foramen, the exoccipital is grooved, presumably for vessels that exited via the posterior lacerate foramen.

Basioccipital: Broken and compressed bone obscures some details of the basioccipital; sutures with the exoccipital

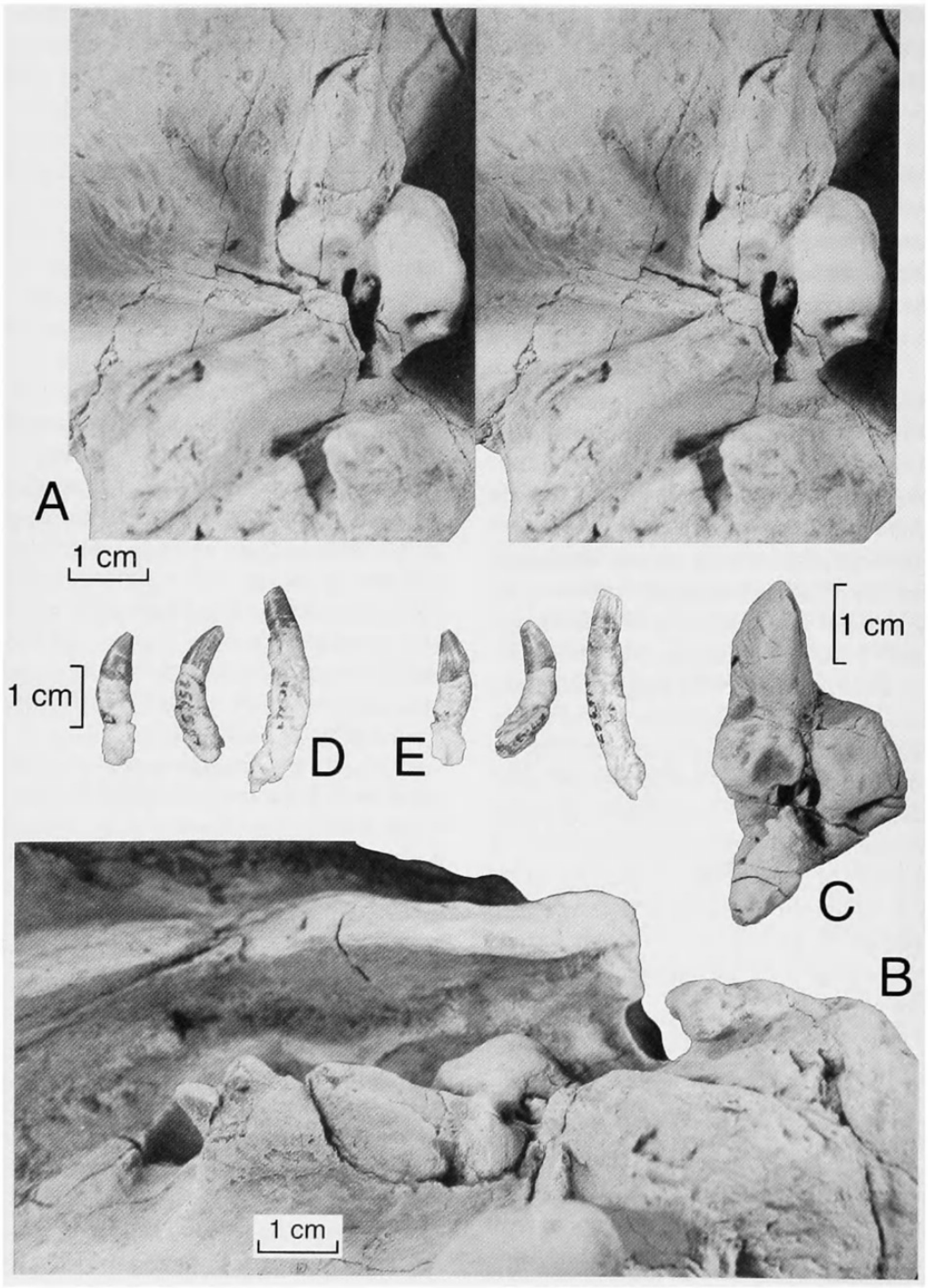

FIGURE 14.—*Simocetus rayi,* USNM 256517, holotype elements, and unnamed odontocete USNM 205491: A, stereophotographs of right periotic of holotype skull of *S. rayi,* USNM 256517, ventral view (skull whitened with ammonium chloride); B, lateral view of right periotic of holotype skull of *S. rayi,* USNM 256517, with ventral surface upper (skull whitened with ammonium chloride); C, right periotic of unnamed odontocete USNM 205491, to show anteroexternal sulcus and posterior process; D,E, isolated anterior teeth associated with holotype skull of *S. rayi,* USNM 256517; D, buccal view; E, lingual view. (Scale bar=1 cm.)

are fused except at a crushed contact at the posterior of the basioccipital crest. The right basioccipital crest is robust and anteroposteriorly short, reaching forward to about the mid-level of the foramen ovale. Its current posteroventral and markedly lateral orientation probably reflects postmortem crushing; originally the crest extended farther ventrally and less posteriorly or laterally, with the posterior lacerate foramen better exposed to ventral view. Rough bone medially near the thickened apex of the crest probably marks the insertion for the longus capitis. Anteriorly, the basioccipital contacts the vomer medially; laterally, the basioccipital crest carries a small, narrow, oval facet interpreted as the suture for the medial lamina of the pterygoid.

An indistinct tubercle lies medially at the contact with the vomer, anterior to a gentle elevation that runs transversely between the bases of the two basioccipital crests. Posteromedially, bilateral ridges that flare back toward each condyle delimit the insertions for the rectus capitis ventralis.

Dorsolaterally, opposite to the periotic, the basioccipital crest lacks any obvious fossa for a peribullary sinus, although such a sinus probably was present. Dorsally, near the border for the posterior lacerate foramen, the basioccipital carries a narrow elongate shelf and an associated groove; because the region between the tympanic bulla and basioccipital is equivalent to the petro-occipital canal of other mammals, the groove may be for the ventral (inferior) petrosal sinus.

The basioccipital contributes little to the margin of the laterally directed posterior lacerate foramen (=cranial hiatus in part of Fraser and Purves, 1960; see Fordyce, 1994), which otherwise is bounded by the exoccipital (posterior) and, particularly, the parietal (lateral). The foramen is long and narrow (~20 mm × ~10 mm), and anteriorly it is confluent with the much larger foramen ovale. Presumably the foramen transmitted cranial nerves IX–XI and any vessels from the sigmoid sinus. The region ventral to the posterior lacerate foramen includes the tympano-occipital fissure and jugular foramen of other mammals, now indistinct because the bulla and periotic are effectively extra-cranial, displaced ventrolaterally from the braincase.

Squamosal: The squamosal appears to form the posterolateral wall of the temporal fossa at and posterior to a prominent bulge in the braincase, although the parieto-squamosal suture cannot be localized here. A long, deep, narrow cleft in the dorsal surface of the squamosal floors the temporal fossa and separates the braincase from the zygomatic process (Figure 2A, right side). Anteroventrally, the cleft is particularly narrow, confined anteriorly by the convex subtemporal crest and by the medial edge of the zygomatic process, as if to form a channel for a tendinous part of temporalis.

The zygomatic process of the squamosal parallels the skull axis and forms the most lateral part of the skull (dorsal view; Figures 2A,B, 3, 4). Its dorsal crest is abruptly rounded transversely, and the medial wall is steeper than the lateral. The zygomatic process is deeper than it is wide, with a roughly comma-shaped cross section, and the thin ventral margin extends a little laterally. In lateral view (Figures 8A, 9), the dorsal margin of the process is subhorizontal, descending gently to a sharp apex below which is an elongate small facet for the contact with the jugal.

Posteriorly, the base of the zygomatic process has a deep, rough fossa for muscles of the neck. Subdivisions are not obvious; the muscles included some or all of the sternomastoideus, splenius, longissimus capitis, and mastohumeralis (see Schulte and Smith, 1918; Howell, 1927). The fossa extends anterodorsally above the external auditory meatus, is pitted deeply in its midpoint, and extends ventrally onto the post-tympanic process of the squamosal (lateral view; Figure 8A). By analogy with artiodactyls, the post-tympanic part of the fossa is inferred to be an origin for the sternomastoideus.

The ventral surface of the squamosal is complex. The lateral edge of the zygomatic process has a marked crest, but limits to the glenoid cavity otherwise are not clear except at the robust postglenoid process. Here the tympano-squamosal recess for the middle sinus (fide Fraser and Purves, 1960) descends onto the postglenoid process, with the distal part of the recess bounded by a distinct ridge on the anterolateral part of the postglenoid process (Figure 5A). Although there is no excavated tympano-squamosal recess anteriorly, the structure of the squamosal between the zygomatic process and steep-sided falciform process is compatible with a well-developed middle sinus (sensu Fraser and Purves, 1960) originating at the lower tympanic aperture between the periotic and tympanic bulla. Farther anteriorly (Figure 5A), the squamosal forms a broad shelf on which a thick rounded subtemporal crest ("projecting...temporal rim" of squamosal, of Kellogg, 1936:101) separates the temporal fossa from the basicranium. As in *Waipatia maerewhenua,* the squamosal lacks the anterior transverse ridge and the vestigial (nonpatent) postglenoid (retroarticular, retroglenoid) foramen seen in Basilosauridae; see also the discussion of postglenoid foramen and foramen spinosum below.

Anteriorly, between the pterygoid sinus and the groove for the mandibular nerve, the alisphenoid-squamosal suture is foliate and complex, with multiple fine interdigitation.

The falciform process is thin, with a long base; it projects ventrally, skewing slightly anteromedially, and is bifurcated distally. On the skull in modern odontocetes in which the tympanic bulla is articulated (e.g., growth series of *Tursiops truncatus* (Montagu) in USNM), the anteroventral or distal part of the falciform process lies close to the descending anterior edge of the outer lip of the bulla. This distal part is missing in *S. rayi,* presumably through postmortem loss. A second, more anterodorsal, division of the falciform process often is identifiable in odontocetes, immediately ventral to the path of the mandibular nerve. This division may contact the bony lateral lamina of the pterygoid sinus fossa. There no evidence that any extensive sheet of outer lamina of pterygoid contacted the falciform process in *S. rayi*. Posteriorly, the falciform process lies closely against the anterolateral face of the anterior process of the periotic, but farther posteriorly, the squamosal rises rapidly to expose much of the anterior process of the periotic to lateral view (Figures 14B, 16). A large foramen between the squamosal and the fovea epitubaria of the periotic, immediately anterior to the lateral tuberosity, marks the ventral opening of the anteroexternal sulcus, which in turn is presumably for the middle meningeal artery (see Fordyce, 1994). The in situ periotic obscures the squamosal within the periotic fossa.

The external auditory meatus is more deep than wide distally, with the anterior and posterior walls roughly parallel for the distal half of its length, and is bounded by the steep posterior face of the postglenoid process. Medially, the meatus is more open and is separated from the tympano-squamosal recess by a

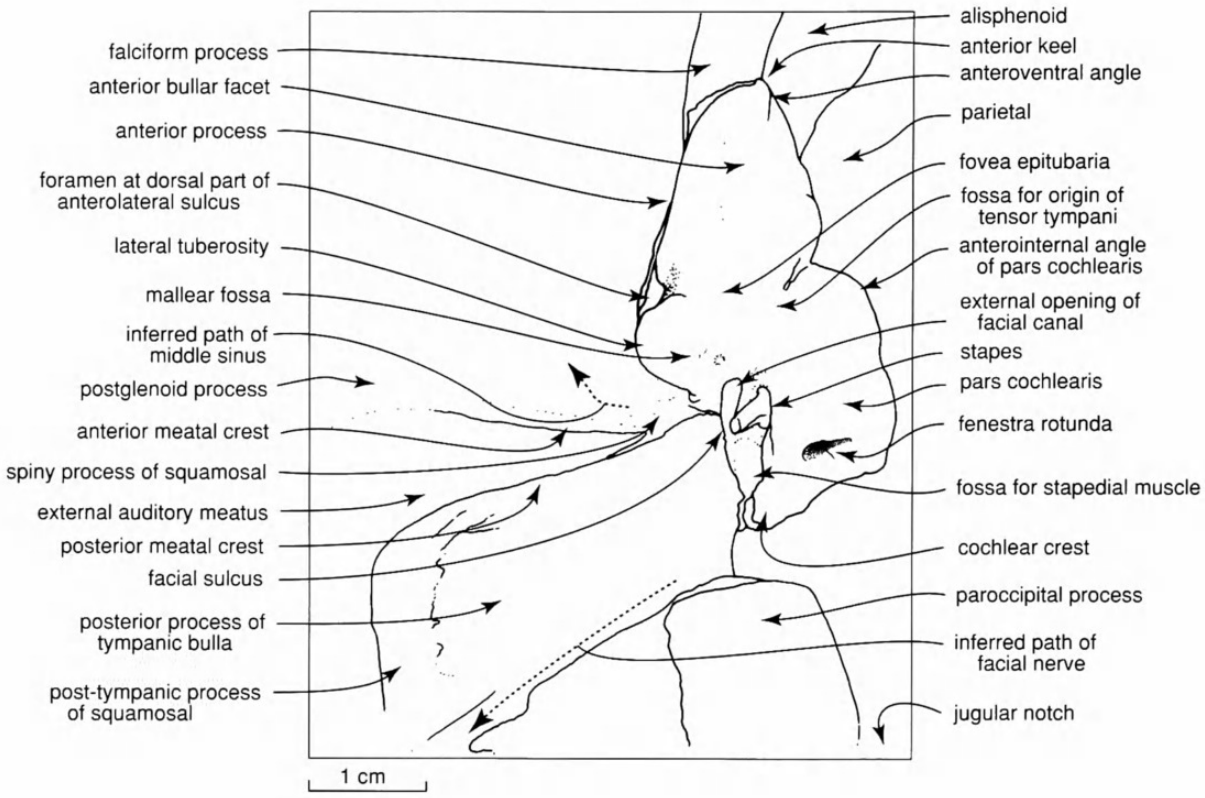

FIGURE 15.—*Simocetus rayi*, USNM 256517, ventral view of right periotic of holotype skull, based upon Figure 14A, showing main features. (Scale bar=1 cm.)

sharp anterior meatal crest. The latter extends from the postglenoid process to the apex of the spiny process (sensu Muizon, 1987), in the hiatus epitympanicus of the periotic, immediately posterior to the lateral tuberosity (Figures 14A,B, 15, 16). Here the spiny process of the squamosal carries two grooves, of which the anterior marks the path of the middle sinus and the posterior is the meatus. The suture between the squamosal and tympanic bulla here is obscure, but the posterior meatal crest forms at least the dorsal few millimeters of the wall of the meatus, with the rest formed by the posterior process of the bulla. The latter covers the squamosal that is presumed to have a post-tympanic process comparable to that of *Waipatia maerewhenua*. The amastoid state of the skull (posterior process of the periotic not visible on the skull wall) is consistent with the interpretation of a substantial post-tympanic process.

Periotic: The right periotic (Figures 14A,B, 15, 16) is preserved in situ and is applied closely to the squamosal (lateral, anterior), alisphenoid (anterior), parietal (anteromedial and medial), exoccipital (posterior), and tympanic bulla (posterolateral and ventral). There is no clear evidence of original intimate sutural contact with these elements, other than at and near the posterior process of the bulla. Details of the lateral and dorsal surfaces of the periotic cannot be seen.

The anterior process, body, and pars cochlearis are all skewed anteromedially relative to the skull axis. The anterior process is about as long as the body, is more narrow than deep, and has a convex lateral face and flatter medial face. As viewed medially, the anterior process is dorsoventrally deepest near its apex. Also, the anterior keel is curved as seen in medial view, with the anteroventral angle apparently more rounded than the anterodorsal angle, which, together with the medial face, is prolonged dorsomedially. The anterodorsal angle approaches a groove (at the parietal-alisphenoid suture) interpreted to lead toward the foramen spinosum. There are several subhorizontal fine grooves (anterointernal sulci of Fordyce, 1994) ventrally on the medial face of the anterior process, and one of these may be for the lesser petrosal nerve. Another groove traverses the medial face toward the anterodorsal angle. Fine details on this face of the periotic (e.g., presence or absence of a vertical canal) are obscured by resistant adhering matrix. Posteriorly, the medial face of the anterior process meets the perpendicular face of the pars cochlearis at an open groove; a fissure, which in odontocetes commonly accompanies an inflated pars cochlearis, is absent. Fordyce (1994) and others, following Kellogg (1936), have interpreted the grooved contact of the anterior process with the pars cochlearis as representing the origin for the tensor tympani; however, it seems likely that the origin for the tensor tympani lies farther ventrally, within the shallow and more subhorizontal groove between the fovea epitubaria and the ventral surface of the pars cochlearis. A long (~9 mm), shallow, grooved anterior bullar facet lies on the ventral surface of the anterior process. The facet is bounded posteriorly by a wide shallow fovea epitubaria for the anterior pedicle and accessory ossicle of the bulla. The fovea is slightly deeper later-

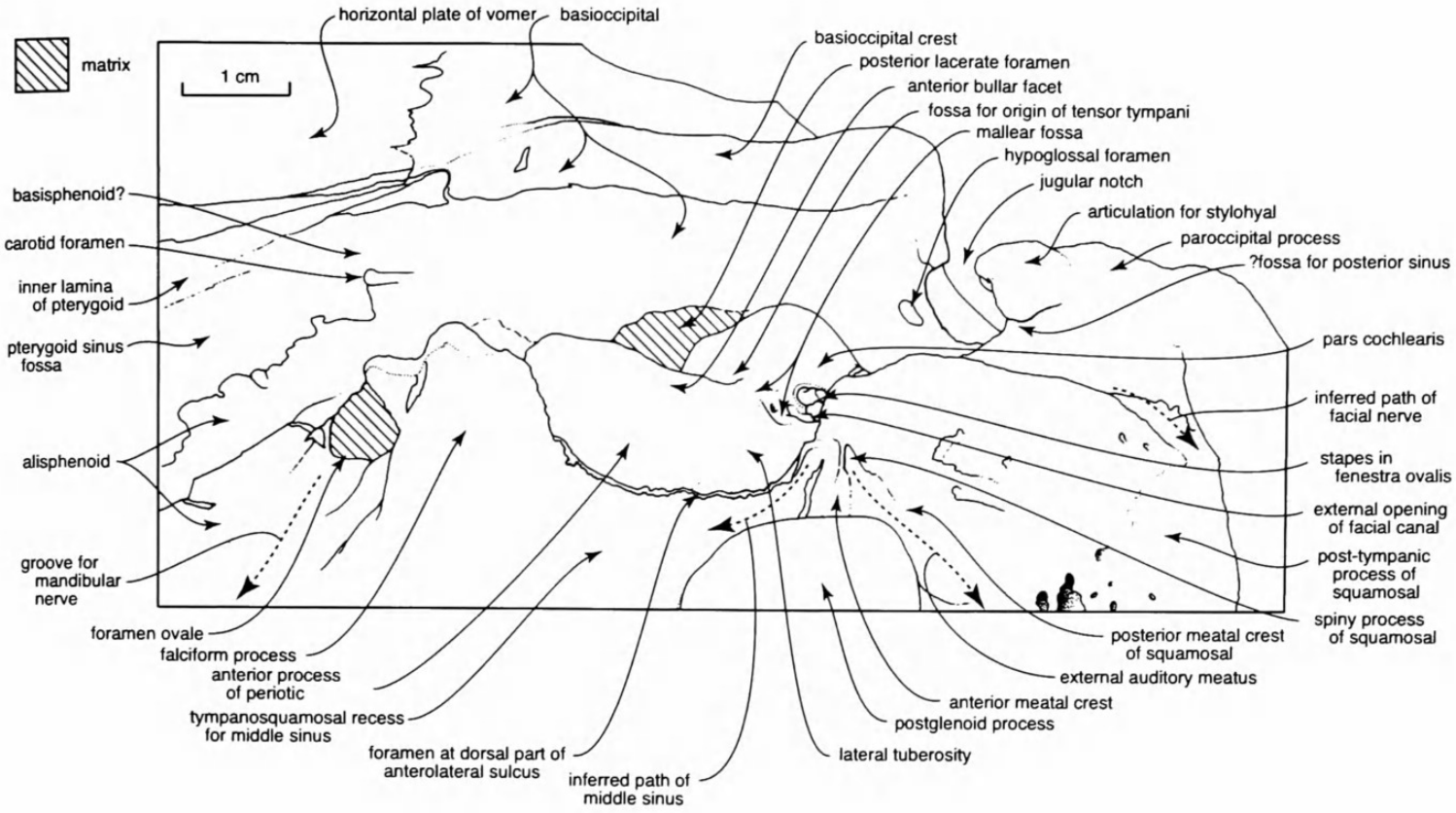

FIGURE 16.—*Simocetus rayi,* USNM 256517, lateral view of right periotic of holotype with ventral surface upper, based upon Figure 14B, showing main features. (Scale bar=1 cm.)

ally, where it is succeeded by the prominent dorsal end of the anterolateral (or anteroexternal) sulcus. The indistinct ventral part of this sulcus is curved, as seen also in some platanistoids and eurhinodelphinids. Comparisons with other archaic Cetacea (e.g., *Zygorhiza kochii* (Reichenbach), *Waipatia maerewhenua,* and archaic odontocete USNM 205491 of Figures 5B, 14C) suggest that this groove, bounded laterally by the squamosal, trends toward the anterodorsal angle on the anterior process of the periotic and marks the path of the middle meningeal artery.

The body is delimited anteriorly by the lateral tuberosity and by the transverse ridge that anteriorly bounds the mallear fossa. The latter ridge is indistinctly tuberculate both medially and laterally, and its relationship with the now-lost anterior pedicle of the bulla is uncertain. Posterodorsally, the large hemispherical lateral tuberosity is undercut deeply. An indistinct facet on the ventrolateral face of the tuberosity probably marks the point where the sigmoid process of the bulla originally lay close to the periotic. The irregularly subspherical mallear fossa is shallow and large, deepest dorsomedially, and faces obliquely posteroventrally. Medially, the fossa merges smoothly onto the pars cochlearis without an obvious groove. There is no distinct fossa incudis, although whether this is an original absence or a postmortem loss is uncertain. The spiny process of the squamosal and, posteriorly, posterior process of bulla, obscure the hiatus epitympanicus. The fenestra ovalis, with in situ stapes, faces posterolaterally and ventrally; its anterior margin is just visible in a lateral view from the skull margin into the external auditory meatus (Figures 14B, 16). The facial canal opens lateral and just anterior to the fenestra ovalis. Because of broken bone, details are uncertain about the facial sulcus (groove for facial nerve), the deep fossa for the stapedial muscle, and the condition of the tympanohyal. The stapes is unrevealing.

The pars cochlearis is long and narrow, is not inflated, and has a smooth, somewhat tabular ventral surface. Its narrow anterior face passes via a rounded anterointernal angle onto the long, steep, irregular medial face. There is a sharp posterointernal angle. The gently concave posterior face is prolonged ventrolaterally into a laterally compressed, blunt, posterior cochlear crest (new term) that closely approaches the posterior process of the bulla. Laterally, the pars cochlearis rises abruptly toward the fenestra ovalis but does not obscure the latter from ventral view. Posteriorly, the indistinctly reniform fenestra rotunda is only just visible to ventral view. A slight nodule at the dorsal lip of the fenestra rotunda merges into a ridge directed toward the presumed position of the aperture for the cochlear aqueduct.

The posterior process of the periotic is directed laterally, as seen from the jugular notch, but is not exposed on the skull wall; hence, the skull is amastoid. There is no evidence on the skull wall of a mastoid foramen.

Tympanic Bulla: Most of the bulla is missing. The long, narrow, posterior process of the bulla is directed posterolaterally, forming the ventral part of the posterior wall of the external auditory meatus (Figures 14A, 15). The proximal two-thirds of the process has a smooth crest that separates the rounded anterior surface from the tabular posterior surface. There is no obvious groove for the facial nerve on the bulla, and there is no stylomastoid foramen laterally; rather, the facial nerve probably lay in the groove between the posterior process of the bulla and the paroccipital process. Laterally the process thins to a distal apex. Sutures between the dorsal surface of the posterior process and adjacent elements, which can be localized to within a few millimeters, indicate contacts similar to those in *Waipatia maerewhenua* and other archaic odontocetes (e.g., Squalodontidae, Eurhinodelphinidae), namely, with the posterior meatal crest anteriorly, with the posterior process of the periotic posteriorly, and with the post-tympanic process of the squamosal laterally.

Pterygoid and Fossa for Pterygoid Sinus: The pterygoid lines part of the fossa for the pterygoid sinus, and it forms a prominent hamulus. Unsurprisingly, delicate parts of the pterygoid are absent; the bone is inferred to have had lateral, ventral, and medial laminae (sensu Fraser and Purves, 1960), which mostly were lost postmortem. The long left hamulus, skewed to the right after death, forms the ventral extremity of the skull just below the level of the palate and basicranium. Ventrally, the transversely rounded anterior surface of the hamulus passes back into a broad-based conical distal portion, broken apically. Although this distal part is dorsoventrally compressed, it is robust and not invaded by the pterygoid sinus. The hamulus extends posteriorly at least to a level with the falciform process. Originally, the medially apposed hamuli formed a prominent posterior spine on the palate.

More-lateral and more-dorsal features of pterygoid are interpreted next in terms of the pterygoid sinus fossa, which here is a large, dorsoventrally deep, compressed cavity lateral and, in part, ventral to the choana (Figures 2B, 4, 8E, 11–13). Remnants at the hamulus indicate that the medial lamina of the pterygoid arose from the anterior half of the hamulus to flank the internal naris at the nasopharyngeal surface. A facet on the anterior face of the basioccipital crest (Figures 4, 5A) indicates that the medial lamina of the pterygoid extended posteriorly to contact the basioccipital, as in other odontocetes. Judging from the remnant of preserved profile at the hamulus, the eustachian notch opened at a level slightly posterior to the midpoint of the pterygoid sinus fossa. Part of the fossa for the pterygoid sinus invades the base of the hamulus, so that in life the sinus underlay the external half of the narial passage. A remnant of ventral lamina arises from the hamulus; in life, the ventral lamina probably extended outward to merge dorsally into the lateral lamina of the pterygoid. Remnants of the lateral lamina occur at the suture with the palatine (at the anterior of the pterygoid sinus fossa) and dorsally along the outer margin of the sinus fossa. A broken surface of lateral lamina indicates a posterior extent at least to the point where the subtemporal crest bulges laterally away from the adjacent pterygoid sinus fossa, and it is possible that the lamina reached farther back, to within 30 mm of the falciform process. The indifferently preserved thin dorsal lamina of the pterygoid forms the anterior and anteromedial roof of the oval elongate sinus fossa, with the alisphenoid forming the posterolateral surface. Anteriorly, the fossa is excavated dorsally above the level of the foramen ovale and subtemporal crest, but it is shallower posteriorly. A small foramen (diameter ~2 mm) placed medially near the apex of the fossa may be the pterygoid foramen, which opens dorsally into the foramen rotundum (Figure 13). The dorsal roof of the fossa, in the region of the pterygoid-alisphenoid suture, possesses many small foramina. Posteriorly, the fossa is bounded by a low ridge that marks the path of the mandibular nerve (V3) from the foramen ovale. There is no evidence that the pterygoid sinus extended beyond the skull base and into the orbit, or that it had medial or posteromedial lobes.

Alisphenoid: Most sutures of the alisphenoid are fused or obliterated, and their limits are determinable only to within a few millimeters. The foramen ovale identifies the posterior border of the alisphenoid. The alisphenoid also forms the posterior and posterolateral parts of the roof of the pterygoid sinus fossa (Figures 5A, 12, 13). The large subcircular foramen ovale is not occluded posteriorly by the parietal and basioccipital, so it is confluent posteriorly with the cranial hiatus. The posteromedial limit of the alisphenoid is indicated by the carotid foramen in the adjacent basioccipital. Relationships with the squamosal are uncertain because they are obscured by complex sutures; the alisphenoid apparently forms only a small medial part of the groove for the mandibular nerve. A splint of alisphenoid extends posteriorly between the squamosal and parietal to reach the anterodorsal angle of the anterior process of the periotic (Figure 5A). The deep groove here between the parietal and alisphenoid is real, not a postmortem artifact; its position and orientation, and comparisons with other odontocetes (*Waipatia maerewhenua* and the unnamed odontocete USNM 205491 of Figure 5B), suggest that it is a fissure for the middle meningeal artery and that its anterior limit represents the foramen spinosum.

Basisphenoid: The carotid foramen, which opens level with but ventromedial to the foramen ovale, indicates the posterior extent of the basisphenoid (Figures 12, 13). Limits to the basisphenoid otherwise are obscured by the vomer ventrally, and by the inner lamina of the pterygoid laterally. The carotid foramen is small and elongate. This foramen is thought not likely to transmit an internal carotid artery in adult living mysticetes and odontocetes (Fraser and Purves, 1960; Vogl and Fisher, 1981), although an artery may be present in juveniles (Melnikov, 1997).

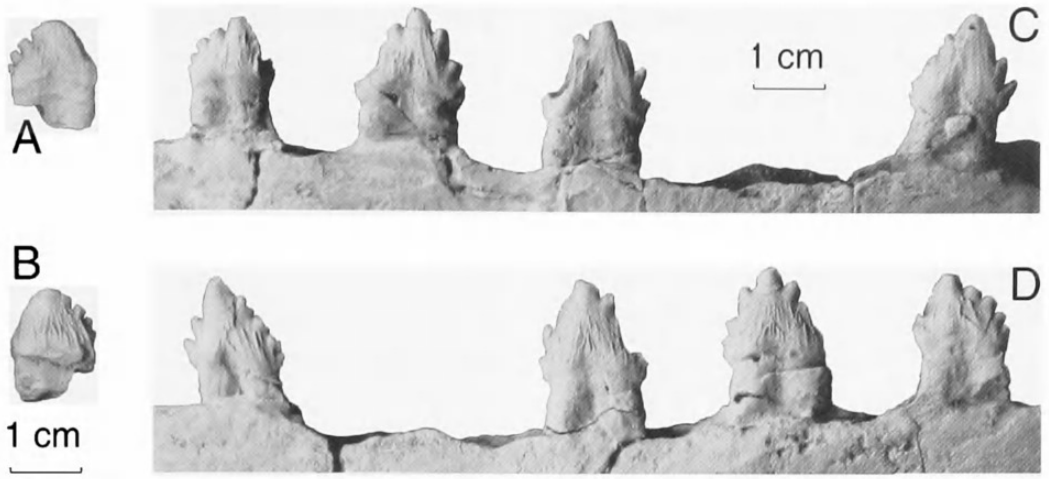

FIGURE 17.—*Simocetus rayi,* USNM 256517, teeth, whitened with ammonium chloride: A,B, isolated crown of a cheek tooth; A, buccal; B, lingual; C,D, mandibular teeth; C, buccal; D, lingual. (Scale bar=1 cm.)

Orbitosphenoid: Details are seen best in the left orbit (Figures 11–13) in which, however, proximal parts of foramina could not be exposed fully. Kellogg's (1936, fig. 31c) illustration of *Zygorhiza kochii* helps interpret this region. The orbitosphenoid surrounds much of the elongate deep cleft of the optic infundibulum but cannot be identified positively in the anterior wall. The optic foramen opens anteriorly in the roof of the infundibulum, which is level with but posteromedial to the ethmoid foramen. The path for the optic nerve is perpendicular to the condylobasal axis. The orbital fissure (=portion of optic foramen for V1 of Kellogg, 1936, fig. 31c) is not seen, but it is inferred to open farther posteriorly, deep within the infundibulum. A small foramen presumably for the ophthalmic artery lies at the junction of the orbitosphenoid, frontal, and parietal, immediately dorsal to the optic infundibulum. Also on the orbitosphenoid is the path of the maxillary nerve (V2) that arises from the foramen rotundum (hidden) and runs anteriorly in a shallow groove that is lateral and ventral to the deeper part of the infundibulum. A low horizontal ridge bounds the groove dorsally, and the ventral edge of the groove is close to the suture with the palatine.

Mandible: Notable features of the incomplete right mandible (Figures 8B,D, 10A,B, 17C,D include its gracile, laterally compressed and ventrally deflected anterior portion, and ventrally and laterally inflated panbone (lateral wall of the mandibular foramen). There are alveoli for 11 teeth, presumably i1–3, c, p1–4, and m1–3. Missing are the apex of the coronoid process, maxillary notch, condyle, condylar crest, angular process, and angle.

Anteriorly, the tooth-bearing body has a sharp apex that passes back into the subparallel dorsal and ventral surfaces. Depth increases markedly about the level of m1–m3, as the panbone becomes laterally and ventrally inflated. The dorsal profile behind the posteriormost cheek tooth is barely elevated above the level of tooth insertion, but not enough of the dorsal profile remains to judge the shape of the now-missing apex of the coronoid process. In dorsal view, the mandible becomes inflated posterior to about m3. Overall, the mandible is suboval in cross section, although the crests are developed anteroventrally below about i1–c; posterodorsally, a sharp, narrow coronoid crest is developed behind m3. The apical 85 mm of the mandible, from p1 forward, is deflected ventrally to complement the inferred original profile of the now-distorted rostrum.

In dorsal view, the mandible is roughly straight except anteriorly where it is slightly recurved medially toward the symphysis. A left mandible, if reconstructed to comparable profiles and articulated with the right, would result in an acutely pointed lower jaw with a narrow mandibular space. Proportions of the rostrum, however, point to a broader mandibular space. It thus seems likely that the orientations of the mandible and symphysis were distorted postmortem.

The mandibular symphysis is short, indistinct, and not particularly prominent in dorsal or internal views. It extends from the apex of the mandible posteriorly to about level with the alveolus of i3. Surface detail is too poor to tell patterns of symphyseal ridges and grooves, if any. There is no evidence that the left and right mandibles were fused.

Four single alveoli with prominent diastemata occupy the anterior 67 mm of the mandible. These, and the alveolus for p1, lie toward the lateral (buccal) face of the mandible, whereas the more-posterior alveoli are on the dorsal surface. The forward-pointing tiny alveolus for i1 lies ventral to the apex. Much larger alveoli for i2 and i3 are suboval and directed anterolaterally, so that these teeth probably were procumbent. A more rounded alveolus for the canine indicates a more vertically oriented, single-rooted tooth. Here and farther posteriorly, there are no alveolar juga. A fine longitudinal ridge links the medial (lingual) margins of the alveoli.

Two-rooted alveoli lie farther posteriorly; the seventh and ninth through 11th teeth (p3, m1–3) are in situ (Figure 17C,D). The shortest diastemata are between p1 and p3; posteriorly thereafter, the diastemata lengthen enough to have accommo-

dated the crowns of opposing maxillary teeth. Poorly preserved shallow pits in the diastemata may be embrasure pits for the apices of upper cheek teeth. Five small elongate mental foramina open on the buccal face (Figure 10A) between i2,3, level with the anterior of p2, level with the anterior of p4, level with the anterior of m2, and between m2,3.

Only the crushed anterior margin of the mandibular foramen is preserved. As viewed laterally, the pan-bone is markedly inflated ventrally, relative to the rather straight dorsal profile between p1 and the broken base of the coronoid process. As seen posteriorly, the medial (lingual) face of the mandible is gently concave. The mandibular canal is at least 70 mm deep and 20 mm wide, and its walls are less than 1 mm thick.

Teeth: The teeth (Figures 14D,E, 17A–D) are heterodont and apparently not polydont. The tooth complement appears to be I0/3, C1/1, P4/4, M2/3, based upon the count of teeth, roots in place, and the alveoli, with the proviso that anterior alveoli are eroded and the matrix is filled. There is no evidence of deciduous teeth. It is uncertain whether premolars and molars can be differentiated on the basis of crown structure; in this specimen they are identified by position. Premaxillary teeth are not recognizable and, furthermore, each premaxilla lacks alveoli. Teeth preserved in the skull (Figure 2B) are the right P4 and M1, left P2, and roots of left P3 and M1; none of these upper teeth is preserved well enough to warrant detailed illustrations. Mandibular teeth are listed above. Isolated teeth are three anterior teeth (i and/or c; Figure 14D,E), one cheek-tooth crown (perhaps left m1; Figure 17A,B), and a fragment of one cheek-tooth crown.

The isolated, slender, single-rooted teeth with simple crowns are incisors and possibly a canine. All are rather small in absolute size and also in size relative to the mandible. The longest, with a relatively small crown, may represent the procumbent lower right i2, for which the alveolus is large and directed forward. Of the two smaller teeth, the straighter is perhaps the lower left i3; the more recurved could represent the lower left or upper right C. In each single-rooted tooth, the crown is acutely pointed with a small apical angle (sensu Rothausen, 1968), is recurved slightly to markedly lingually, and is anteroposteriorly keeled. The basal cross section is oval and transversely compressed, and the buccal face is more convex than the lingual face; transverse compression is pronounced apically. The enamel is smooth or has microscopic vertical striae buccally, whereas the lingual face has a few low, vertical, subparallel ridges. In each tooth, the root has a smooth surface, is thicker below the crown, and is roughly circular in cross section.

Features of the cheek teeth are shown in Figure 17A–D. On the skull, only the right P4 appears to be in undistorted original position, facing ventrally and slightly laterally (buccally) (Figure 8A). The cheek teeth in place are emergent, with the crown well clear of the alveolus. Generally, the triangular crowns are laterally compressed, are recurved lingually in the upper teeth, and have a triangular main (apical) denticle and two or more accessory (anterior and posterior) denticles. In other archaic odontocetes, the apical denticle becomes smaller posteriorly in the tooth row relative to the accessory denticle(s); in *S. rayi* the apical denticle in the lower p3 is larger than in the m1, but more teeth are needed to determine the real trend. Accessory denticles are small, compressed, free-standing, and keeled. They are arranged anteroposteriorly along the keels of each tooth. In the lower teeth, an occlusal view shows that this arrangement is roughly linear, but for the upper teeth, the anterior and posterior keels, and their associated denticles, trend buccally as they descend from the main denticle. Some accessory denticles are preserved well enough to show apical wear. There are large facets on the left P2 (anterolingual face), right M1 (anterobuccal edge), m1 (posterior keel), m2 (posterior keel), and on the isolated crown, resulting from tooth-to-tooth wear that has removed denticles. The right m3 lacks large anterior denticles and is clearly asymmetrical in lateral view. Anteriorly, the keel on m3 carries a flat face bounded by two distinct ridges, similar to the anterior vertical groove bounded by ridges in the lower molars of basilosaurids (see Kellogg, 1936:124–125).

Ornament is present on all cheek teeth, less marked buccally than lingually. The buccal ornament (Figure 17C) comprises coarse, low, broad-based ridges that arise in the midline toward the crown base and converge apically toward the main denticle. The ridges are shorter and coarser basally. The buccal ornament is most pronounced on the posterior mandibular teeth. The lingual ornament (Figure 17D) is more raised, is longer, has sharper crests, and is distributed farther apically and anteroposteriorly along the crown than for the buccal ornament. A faint papillate cingulum, in the shape of an inverted open V, is present lingually on lower m2,3. There is no cingulum on the more-anterior lower cheek teeth or the in situ upper cheek teeth, although ornament is more pronounced toward the crown base as if forming an incipient cingulum. In all cheek teeth, a vertical median sulcus extends onto the crown base buccally and lingually from between the roots, so that a cross section near the crown base has a compressed figure-8 shape. The enamelocementum boundary varies in profile (lateral view) from gently convex apically to an inverted V shape, with the apex of the V marking the median sulcus on the crown base.

Cheek-tooth roots are subparallel and fused for all of their exposed length out of the alveoli. In the slightly displaced upper left P2, the exposed roots curve posteriorly. The right P4 has what may be a lingual third root, fused to the face of the posterior root and skewed posteriorly into the alveolus. Some roots have a prominent basal swelling near the crown base. Roots of the right P4 and M1 also have conspicuous lines, presumably growth lines, on the cementum parallel to the surface of insertion in the alveolus.

Discussion of Morphology, Homology, and Function

The skull of *Simocetus rayi* helps us understand the early evolution of cranial functional complexes in odontocetes. Previously, patterns of odontocete cranial evolution have been inferred mainly from Neogene and living odontocetes (Miller, 1923; Kellogg, 1928). The few archaic odontocetes described, such as *Agorophius pygmaeus* (Müller, 1849) and *Archaeodelphis patrius* Allen, 1921, have given tantalizing glimpses of primitive morphologies, which, however, need to be put into modern context. For *Simocetus rayi,* the functional complexes discussed below are the face, olfactory complex, orbit, feeding apparatus, and basicranium.

Face: *Simocetus rayi* may be interpreted in light of the facial structure in living odontocetes. In odontocetes, the unique posteriorly expanded supraorbital or ascending process of the maxilla (Winge, 1921; Miller, 1923) forms an origin for hypertrophied maxillo-naso-labialis (nasofacial) muscles (Lawrence and Schevill, 1956; Schenkkan, 1973; Mead, 1975; Heyning, 1989; Curry, 1992). Nasofacial muscles and the associated nasal diverticula and melon are thought to produce and transmit high frequency sounds used in echolocation (Mead, 1975; Wood and Evans, 1980; Heyning, 1989; Cranford et al., 1996). On the basicranium, the pterygoid sinuses may help receive and process high-frequency sounds (Norris, 1968). Mysticetes lack an odontocete-like supraorbital process of the maxilla; they also lack hypertrophied nasofacial muscles, nasal diverticula, and a large melon (Heyning and Mead, 1990). Further, mysticetes are not known to produce and use high-frequency sounds in the manner of odontocetes (Heyning and Mead, 1990).

The face of *Simocetus rayi* shows some broad sutural and topographic patterns similar to those of extant odontocetes. Indeed, such features are critical in identifying *S. rayi* as an odontocete. Furthermore, the skull structure points to *S. rayi* as having essentially the same facial soft tissues as are seen in extant odontocetes. Below is a generalized summary about facial structures in living odontocetes that might also apply to *S. rayi.* This summary is based upon Lawrence and Schevill (1956), Moris (1969), Schenkkan (1973), Schenkkan and Purves (1973), Mead (1975), Heyning (1989), Curry (1992), and Cranford et al. (1996).

In odontocetes, the external nose is a dorsal single blowhole, generally median and well posterior to the apex of the rostrum. Complex nasal diverticula are developed in the soft tissues of the face between the blowhole and the skull. Generally, for the nasal diverticula, it is only the premaxillary sac that has a distinct bony origin (on the premaxillary sac fossa). Proximally, nasal plugs occlude the nasal passages at the external nares.

Nasofacial muscles originating from the premaxilla, and particularly the maxilla, open and close the nostril (blowhole) and manipulate the nasal diverticula. Nasofacial muscles have distinct origins on the premaxilla (nasal plug muscle), on rostral and facial parts of the maxilla, and on some of the frontal. Posteriorly, the hypertrophied nasofacial muscles commonly occupy a distinct depressed facial fossa, with little, if any, bony differentiation of muscle origins in the facial fossa. Anterior limits of the nasofacial muscles on the rostrum are diffuse. A melon is present anteriorly, although without a consistent discrete bony fossa, so that it is difficult to predict size and shape of the melon from skull form alone.

The premaxillary foramina transmit branches of the internal maxillary artery and the maxillary nerves to parts of the nasofacial muscles anteriorly and posteriorly on the rostrum (see, e.g., Schenkkan, 1973, fig. 5, on *Mesoplodon bidens* (Sowerby)). More posteriorly placed dorsal infraorbital foramina supply branches of the internal maxillary artery and maxillary nerves to the region near the antorbital notch and the facial fossa. There is little bony evidence of venous drainage from the face (Mead, 1975). The odontocete face is innervated by sensory infraorbital branches of the maxillary division (V2) of the trigeminal nerve, which issue from the dorsal infraorbital foramina, and the facial nerve, which passes dorsally to the face via the antorbital notch (Huber, 1930, 1934; Mead, 1975).

Within each bony naris is a diagonal membrane, a soft tissue structure that may have a role in sound production (Mead, 1975). The membrane lies in the posterolateral corner of each bony naris and is inserted at the posterior of the nasal septum distal to small foramina in the mesethmoid that may be a vestigial olfactory foramina or a foramina for the nasal nerve.

The orbit is displaced ventrolaterally to become functionally independent of the rest of the face. Mysticetes and archaeocetes, which lack an enlarged facial fossa, have a similar orbital form, so that such changes probably are not caused solely by development of the nasofacial muscles.

All the above features are inferred for *S. rayi.* There is no reason to think that bone and soft tissues had a fundamentally different structure from that of living odontocetes. Facial topography, detailed suture patterns, and positions of foramina differ from those of living species, however, and require comment. For example, *S. rayi* has a prominent depression laterally on the maxilla immediately anterior to the antorbital notch; this rostral area perhaps held a substantial volume of nasofacial muscles that inserted around the nose. Extant odontocetes, in contrast, have nasofacial muscles arising mainly on the cranium, with a limited rostral component (Mead, 1975; Heyning, 1989; Cranford et al., 1996). *Simocetus rayi* also differs in facial topography in having a long rounded "snout," presumably for a well-developed olfactory complex (discussed below).

The internal and external borders of the premaxillary sac fossa are obvious in *S. rayi,* as in extant odontocetes. The lack of a distinct roughened origin for the nasal plug muscle does not preclude this muscle's presence; the bony origin is indistinct, for example, in the living *Platanista* spp. and mysticetes that have nasal plugs but lack a discrete roughened fossa on the premaxilla. *Simocetus rayi* has only an indistinct prenarial constriction, with the premaxillae barely expanded over the mesorostral groove anterior to the narial opening; a cartilaginous median septum was probably developed here and farther poste-

riorly, to form a median border for the nasal plugs. The premaxillary sacs would have lain anterolateral rather than anterior to the bony nares, with posteromedial rather than posterior openings into the narial cavity. Extant adult odontocetes generally have one, not two, premaxillary foramina, in contrast to *S. rayi,* but double foramina do occur sporadically. For example, an adult of *Lipotes vexillifer* Miller has a second premaxillary foramen in the anteromedian sulcus (AMNH 57333; see also Brownell and Herald, 1972, fig. 1), and neonatal delphinids may show two closely associated premaxillary foramina that become confluent in adults. Two well-developed premaxillary foramina occur in the premaxilla of some extinct odontocetes (e.g., *Patriocetus ehrlichi* (Van Beneden) of Rothausen, 1968, fig. 2a; *Squalodon bariensis* (Jourdan) of Muizon, 1991, fig. 7a). In these fossils, the posterior premaxillary foramen lies within the posterolateral sulcus, as in *S. rayi.*

A posteromedian sulcus, which is well developed at the premaxillary sac fossa of many other odontocetes (e.g., *Lophocetus repenningi* Barnes (1978:4); *Mesoplodon bidens* (Schenkkan 1973:5)), is not obvious in *S. rayi,* but another sulcus, the median premaxillary cleft, is notable. A comparable feature occurs in the fossils *Waipatia maerewhenua* Fordyce, 1994 (holotype OU 22095) and *Lomacetus ginsburgi* Muizon, 1986 (holotype MNHN PPI 104; fissure originally interpreted as a taxonomically important median suture between the premaxilla and maxilla—see Muizon, 1988c:33: "fissure longitudinale"). On the left premaxilla of the unnamed odontocete USNM 299482, the median premaxillary cleft meets the eroded remnant of the posterolateral sulcus at a premaxillary foramen. Similar clefts arise from the premaxillary foramen in some extant odontocetes (*Mesoplodon densirostris* (Blainville), USNM 486173; *Mesoplodon hectori* (Gray), USNM 504260; *Phocoena phocoena* (Linnaeus), USNM 550843 and USNM 550844).

Simocetus rayi differs dramatically from extant odontocetes in the structure of its bony nares. The nasal passages of *S. rayi* are directed obliquely, with the bony nares roofed by long and dorsoventrally thin nasals and frontals, so that the external bony nares are more similar in position and orientation to those of extant mysticetes than to extant odontocetes. The nasal region in *S. rayi* could not be prepared, but some other structures may be inferred. In the unnamed archaic odontocete USNM 299482, which is similar in external topography and bone contacts to *S. rayi,* well-developed turbinal bones (Figure 5D) are exposed in the broken cross section at the posterior of a long nasal cavity (Figure 5E). Vestigial turbinals also occur in mysticetes (Edinger, 1955) and are developed well in archaeocetes (Stromer, 1908); among odontocetes, Squalodontidae may possess small cribriform plates, turbinals, and prominent olfactory peduncles within the cranium (e.g., Dart, 1923, fig. 19; Kellogg, 1928:198–202; Flynn, 1948). Turbinals are inferred, therefore, in *S. rayi.* Also in unnamed archaic odontocete USNM 299482, as in mysticetes and, presumably, *S. rayi,* the external bony nares are rather removed from the anteroposteriorly elongate olfactory cavity and turbinals. In contrast, most Neogene and living odontocetes have near-vertical narial passages, and anteroposteriorly short and nodular nasals that rarely roof the nares, and they lack an capacious olfactory cavity with the turbinals. Small foramina that could be vestigial olfactory foramina are nearly ubiquitous in the mesethmoid of extant odontocetes; alternatively, some of these foramina could mark the path of the nasal nerve and associated vessels. *Simocetus rayi* thus probably had soft tissues of the face that functioned around a snout more similar in shape to that of modern mysticetes than to modern odontocetes.

It is not clear how the prominent snout in *S. rayi* would have constrained the structure and operation of the nasal plugs, the diagonal membrane, and the nasal diverticula. Retracted nasals, a reduced olfactory complex, and development of a roughly vertical narial passage have been regarded as functionally linked to the telescoped odontocete skull (Miller, 1923; Norris, 1968). Structures in *S. rayi,* however, indicate that, during odontocete history, the nasofacial muscles migrated posteriorly first, and the olfactory complex was reduced later.

FACIAL ASYMMETRY.—Bilateral asymmetry at the flared rostral margins of the maxillae and antorbital notches in *S. rayi* is comparable to that in some other archaic odontocetes (*Waipatia maerewhenua, Microcetus sharkovi* Dubrovo, *Squaloziphius emlongi* Muizon) discussed by Fordyce (1994:165). Because this maxillary and rostral asymmetry occurs in a range of archaic odontocetes, it is presumed to be directional, with functional implications, and not merely fluctuating or random asymmetry that might be ascribed to ontogenetic "noise." Bony rostral asymmetry probably reflects asymmetry in overlying muscles, although study of living species does not help to understand which of the rostral muscles are involved (Mead, 1975; Heyning, 1989; J.G. Mead, pers. comm., 2001). Nasal asymmetry is seen in *S. rayi;* the right nasal has a more convex lateral border and blunter posterolateral profile, but whether this is fluctuating or directional asymmetry is uncertain.

Asymmetrical nasofacial muscles and/or nasal diverticula are ubiquitous in living odontocetes (Schenkkan, 1973; Mead, 1975; Heyning, 1989), even those with apparently symmetrical skulls (e.g., *Pontoporia blainvillei* (Gervais and d'Orbigny); cf. Kellogg, 1928, fig. 11, and Schenkkan, 1973, fig. 13). It seems likely that the largely symmetrical *S. rayi* probably also had asymmetrical facial soft tissues.

GRADES OF EVOLUTION OF THE FACE.—The grade of facial structure for *Simocetus rayi* is intermediate between that of the most archaic odontocete described, *Archaeodelphis patrius* Allen, 1921, and the rather more modern *Waipatia maerewhenua* Fordyce, 1994. A comparison between these species helps to understand changes in the grade of evolution of nasofacial muscles. Two other widely cited archaic taxa are not considered in this section but are discussed under "Phylogenetic Relationships," below. One, *Agorophius pygmaeus* (Müller)

(see True, 1907), is known certainly only from a single, now-lost, skull for which details are unknown; it is similar in grade to *S. rayi*. Another, the enigmatic *Xenorophus sloani* Kellogg (1923b), is rather similar to *Archaeodelphis patrius*.

In *A. patrius,* the supraorbital or ascending process of the maxilla extends back little, the orbit is elevated with a prominent infraorbital process of the maxilla, development of a facial fossa on the cranium is minimal, and the dorsal infraorbital foramen lies rather anteriorly about level with the antorbital notch. Such features indicate that the nasofacial muscles originated far anteriorly on the cranium and on the base of the rostrum. Because the supraorbital process of the maxilla extends posteriorly well beyond the facial fossa and dorsal infraorbital foramina, "telescoping" of the maxilla is perhaps more than just a simple response to posterior migration of the nasofacial muscles. Anteriorly, the premaxilla is lost, so that details are not known for the premaxillary sac fossa and associated sulci.

In *S. rayi,* the supraorbital process extends posteriorly toward the orbitotemporal crest but not far laterally over the supraorbital process of the frontal; this condition is presumed to be intermediate between that seen in *A. patrius* and most other odontocetes. The orbit is elevated rather less than in *A. patrius,* the infraorbital process of the maxilla is minimal, and a facial fossa lies above the orbit. Multiple dorsal infraorbital foramina open both on the base of the rostrum near the antorbital notch and on the supraorbital process of the maxilla. Judging from the topography of the supraorbital region, the facial portion of the nasofacial muscles was better developed than in *A. patrius*. The prominent lateral crest on the supraorbital process of the frontal probably marks the limits of origins of the nasofacial muscles; interestingly, a substantial part of the supraorbital origin of the nasofrontal muscles lies on the frontal, rather than mainly on the maxilla. The premaxillary sac fossa and associated sulci lie well anterior to the antorbital notch.

Waipatia maerewhenua shows a more advanced grade, comparable to that of many extant groups: the facial fossa is large; the roof of the shallow orbit is about level with the lateral border of the rostral part of the maxilla, so that the origins of the rostral muscle 5 and facial muscle 5 are roughly on the same plane; and the maxilla does not contribute to the orbit. Well-developed premaxillary foramina and sulci are associated with a broad "spiracular plate" for the premaxillary sac fossa. Fordyce (1994) concluded that *W. maerewhenua,* with facial structure fundamentally the same as in extant Odontoceti, was probably capable of echolocation.

FEEDING APPARATUS.—Teeth in *S. rayi* contrast with the dentitions of archaeocetes in that the teeth are absolutely and relatively small, the cheek teeth are separated by marked diastemata, and the posteriormost cheek teeth are inserted far anterior to the antorbital notch. Such features also occur in the archaic mysticete genus *Aetiocetus* (see Barnes et al., 1995). The tooth complement of *S. rayi* is unusual for an odontocete in that upper incisors are absent and the dentition is not polydont.

The lack of alveoli in the premaxillae suggests that I1–3 either were lost or were tiny and embedded only in the gums. In contrast, upper incisors are well developed in other archaic odontocetes, such as squalodontids and kentriodontids, and in basilosaurid archaeocetes, all of which have three premaxillary teeth. Incisors also occur in archaic mysticetes. In extant odontocetes, functional incisors are retained if functional maxillary teeth also are present. Upper incisors are absent in some living species of odontocete (e.g., *Grampus griseus* (Cuvier) and many Ziphiidae) that lack a functional upper dentition. Among fossil taxa, only eurhinodelphinids reportedly have toothless premaxillae. A special explanation, below, seems warranted for incisor loss in *Simocetus*.

Polydonty, or increase in tooth number above the usual mammalian complement, previously has been interpreted as a synapomorphy for Odontoceti (e.g., Fordyce, 1983a; Barnes, 1990:21, item 10), so that the lack of polydonty in *S. rayi,* an archaic odontocete, is unexpected. All extant Odontoceti, and fossil Odontoceti for which complete dentitions are known, either are polydont or have dentitions plausibly reduced from a polydont condition. For example, *Xenorophus sloani* Kellogg (1923b), perhaps the most archaic odontocete for which the dentition is documented, has 10 maxillary teeth. Among other Cetacea, archaic mysticetes and embryos of some living mysticetes are polydont, whereas archaeocetes and a few archaic mysticetes are not polydont (Kellogg, 1936; Barnes et al., 1995). For *Simocetus,* tooth complement could be plesiomorphic with archaeocetes, or it could reflect a secondary reversal to a nonpolydont state.

The feeding apparatus of *S. rayi* is quite unlike that described for other odontocetes, thereby allowing a novel interpretation of function. Alveolar form for i1–c suggests that these lower teeth were procumbent, with i1 vestigial. Anteriorly, the dorsal surface of the conjoined mandibles at the symphysis is narrow and flat, without teeth that protrude above the jawline, so that the apically downturned mandibles probably occluded against the similarly downturned, flat, edentulous anterior of the palate. Analogs are not seen in other Cetacea, but among Sirenia, Domning (1978) observed that the degree of deflection of the sirenian rostrum appears to correlate directly with the degree to which bottom feeding is used. Sirenia generally lack functional anterior teeth and use horny pads instead to crop and crush vegetation. The apices of the rostrum and mandible are strengthened, the mandible by thickening of the dorsal edges of the horizontal bodies and lateral edges of the masticatory surface (partly developed in *S. rayi*), and the snout by buttressing of the dorsal outline (not in *S. rayi*). Therefore, *Simocetus rayi* may have been a bottom feeder. In view of the relatively delicate cheek teeth and nonbuttressed rostral apex, a durophagous diet (e.g., molluscs) seems unlikely; soft-bodied benthic invertebrates were probably taken.

Further evidence in support of bottom feeding is provided by the presence of indistinct large, shallow, paired pits at the ros-

tral apex, presumed to be for the vomeronasal (Jacobson's) organ. A groove from each pit leads toward the presumed palatine fissure. The vomeronasal organ is a branch of the olfactory complex that is functional in some other mammals (e.g., Evans, 1993) and has been reported in extant mysticetes (Quay and Mitchell, 1971). A vomeronasal organ could have functioned in *S. rayi* as a chemoreceptor in bottom feeding.

The cheek teeth are delicate, with small denticles, and are widely spaced. Occlusal wear is on the anterior (mesial) and posterior (distal) faces, rather than on the buccal or lingual. Carnassial-like shearing seems unlikely; rather, teeth probably functioned in simple grasping or perhaps in a sieve-feeding system like that of the extant crab-eater seal, *Lobodon carcinophagus* (Hombron and Jacquinot) (see King, 1961). The combination of a broad palate, short mandibular symphysis, and long mandibular space indicates a voluminous mouth that could have functioned to hold water during suction feeding or filter feeding. *Simocetus rayi* perhaps fed on small epifaunal or shallow infaunal invertebrates detected with the aid of the vomeronasal organ. Perhaps it was a mud-grubber and used teeth to filter food from a substrate-water slurry.

The long, robust, conical unexcavated proximal portions of the pterygoid hamuli possibly functioned as secondary posterior extensions of the hard palate. Similar long hamuli occur in a few other extinct odontocetes (e.g., unnamed problematic archaic odontocete USNM 243979, the eurhinodelphinids *Eurhinodelphis bossi* Kellogg, 1925, *Argyrocetus joaquinensis* Kellogg, 1932, and the presumed eurhinodelphinid *Squaloziphius emlongi* Muizon, 1991), but the functional significance is not clear. Accounts of the nasopharyngeal muscles in extant odontocetes (Fraser and Purves, 1960) indicate that enlarged hamuli could play a major role in the function of the palatopharyngeal muscles.

FEEDING MUSCLES.—Skull proportions indicate that the temporalis was the largest masticatory muscle, which suggests a simple hinge closure of the mandible as in archaic eutherians, where the temporal is dominant (Turnbull, 1970). The proportions of cranium to rostrum, and to temporal fossa, indicate a lever action of the mandible that was powerful and slow; in contrast, *Waipatia maerewhenua* had proportionally smaller temporal fossa, longer forceps-like jaws, and an inferred faster but weaker snap (Fordyce, 1994). Other features related to the temporalis are puzzling; examples are the long tabular postorbital process (implicated in the action of the temporalis; Perrin, 1975); the straight, long inner face of the zygomatic process; and the deep cleft on the squamosal in the posterior floor of the temporal fossa. The masseter and zygomatico-mandibularis muscles were probably small, given the reduced infraorbital process of the maxilla and the small zygomatic arch of the jugal. The palatine, perhaps aided by the lateral lamina of the pterygoid, formed a large origin for the pterygoid muscles, but there is no evidence of hypertrophied pterygoideus or significant lateral/medial movements of the mandibles in feeding. The paroccipital process is large, potentially providing a large origin for the digastric muscle. Alternatively, large size could relate to articulation of the stylohyal.

ORBIT.—Key features of the orbit are the arched profile extending well above the level of the lateral border of the rostral part of the maxilla, a deep optic infundibulum, an indistinct preorbital ridge, a large infraorbital infundibulum, and a limited contribution of the maxilla to the anterior wall. In archaeocetes, the orbit is arched more strongly, with a more distinct preorbital ridge (so that the sphenopalatine foramen is better separated from the orbit); in contrast, the orbit in Neogene and living odontocetes lies about level with the alveoli and usually is flattened from above by the facial fossa. In archaeocetes, the optic infundibulum is shallower, with contributing foramina placed more posteromedially in a much narrower interorbital region than in *Simocetus;* possibly the depth of the optic infundibulum in *S. rayi* relates to relative interorbital width, although the functional significance of change in interorbital width is uncertain. There is no reason to think that the voluminous optic infundibulum held a rete. *Simocetus rayi* differs from the dorudontine archaeocete *Zygorhiza kochii* (see Kellogg, 1936, fig. 31c) in that the foramen rotundum for the maxillary branch of the trigeminal nerve, V2 (=sphenorbital fissure of Kellogg), opens within the optic infundibulum, together with the optic foramen and orbital fissure. Change in the position of the foramen rotundum relative to other orbital foramina may reflect shortening of the intertemporal region. Mysticetes, which have a shortened intertemporal region, also have a foramen rotundum that opens within the optic infundibulum. The relative importance of the orbital and associated foramina is hard to judge from their size; foramen size in extant Cetacea does not always correlate with size of the nerve or vessel that issues from it, and some foramina may be enlarged through the development of retia (Breathnach, 1960).

In terms of maxillary contribution to the orbit, *S. rayi* is intermediate between archaeocetes and modern odontocetes. In archaeocetes, the maxilla forms the anterior wall of the strongly arched orbit, whereas there is minimal contribution in modern odontocetes. In living species, the orbit and ventral infraorbital foramen are in about the same horizontal plane as the lateral border of the rostral part of the maxilla. The maxilla effectively forms the anterodorsal roof of the orbit. A preorbital ridge (inferior orbital crest) may be present. These changes in the orbital region perhaps reflect the posterior movement of facial muscles and development of an enlarged facial fossa, rather than major changes in eye function.

PTERYGOID SINUS.—Norris (1968) suggested that air sinuses in the basicranium may isolate the auditory region from self-produced sound and may help to channel external sound to the periotic. Therefore, the development of sinuses may give a guide to hearing capabilities. In *S. rayi,* the fossae for the pterygoid sinuses are more derived than those of basilosaurid archaeocetes; they are longer relative to cranial length, extend

relatively farther forward, are relatively more excavated dorsally, and extend ventromedially into the pterygoid hamuli. Relative to modern odontocetes, however, the fossae in *S. rayi* are more primitive in many respects. They do not extend as far anteriorly on the cranium and appear to be relatively smaller than, for example, the superficially similar but large sinus fossae of Ziphiidae and Physeteroidea. Further, the sinuses in *S. rayi* are restricted to the basicranium, in contrast to many other odontocete groups in which the sinuses invade the orbit (Fraser and Purves, 1960) through dorsal expansion, often with loss of a bony wall on the pterygoid sinus fossae.

In *S. rayi,* the alisphenoid forms the posterodorsal and posterolateral parts of the pterygoid sinus fossa, as in basilosaurid archaeocetes and the archaic mysticete *Mammalodon colliveri* Pritchard. None of these cetaceans is preserved well enough to see clearly how alisphenoid relates to the pterygoid at the lateral wall of the fossa.

Of the more-posterior parts of the pterygoid sinus complex, little can be said about the middle sinus, other than to emphasize that bone topography is consistent with the presence of that sinus. Proportions of the peribullary sinus (e.g., volume between bulla and basioccipital) cannot be judged because the tympanic bulla is missing. The basioccipital crest is relatively deeper and narrower than in archaeocetes, possibly contributing to an enlarged fossa for the peribullary sinus. The crest is not excavated to form a thin plate, however, as in some species of Delphinidae, for example.

Concepts of the posterior sinus among odontocetes and mysticetes are confused. Many odontocetes carry a fossa, commonly termed the fossa for the posterior sinus, on the anterior face of the paroccipital process dorsal to the apex of this process. The cavity may be deeply concave, e.g., as in *Phocoena phocoena* and *Pontoporia blainvillei,* or may be shallow but well delimited, as in *Tursiops truncatus*. In many odontocetes, there is a less distinct excavation anteriorly at the apex of the paroccipital process, right at the articulation of the stylohyal and clearly distal to the position of the often more distinct larger fossa. In heads of extant delphinids, injections of the pterygoid sinus complex with silicone rubber (*Stenella longirostris* (Gray), USNM 396173; *Lagenodelphis hosei* Fraser, USNM 396079) revealed that this less distinct excavation carries a small lobe of sinus that originates from the eustachian cavity via the elliptical foramen of the tympanic bulla. This lobe must be the posterior sinus sensu stricto (Fraser and Purves, 1960:9). Accordingly, the subtle fossa that lies more ventrally (more distally), near the apex of the paroccipital process, is the posterior sinus fossa sensu stricto, whereas the cavity that lies more dorsally in the paroccipital process is probably for a lobe of the peribullary sinus.

Overall, structures seen in *S. rayi* give no new insight into the function of the pterygoid sinus system, but they indicate that the basicranial sinuses were comparable in structure and hence function to those of extant odontocetes.

EAR, HEARING, AND BASICRANIAL CIRCULATION.—Comment on these aspects is limited, because the periotic is indifferently preserved and obscures the adjacent squamosal, and because most of the tympanic bulla is missing. The bony groove for the external auditory meatus is primitively larger than the narrow vestigial cleft of most extant odontocetes. Squamosal-bulla-periotic contacts are similar to those of *Waipatia maerewhenua, Notocetus vanbenedeni* Moreno, and the extant *Platanista gangetica* (Roxburgh) (see Muizon, 1987; Fordyce, 1994), judging from the amastoid skull wall and from contact relationships of the posterior process of the bulla with the squamosal at both the external auditory meatus and posttympanic process. It is notable that, in all extant and fossil odontocetes studied during this project, the posterior meatal crest of the squamosal articulates with the anterior face of the posterior process of the tympanic bulla. The articulation is present even in Delphinidae (although very reduced); delphinids commonly are regarded as having the tympanoperiotic disarticulated from the adjacent skull.

Some inferences may be made about cranial circulation in *S. rayi,* but with important provisos: (1) Details of arterial circulation are known reliably for only a few extant species of cetaceans (see below). (2) General features of venous circulation were described by Fraser and Purves (1960; see also their summary of Boenninghaus, 1904), but there are no detailed modern accounts of paths of individual vessels from the cranial cavity to the basicranium. (3) There seem to be no accounts of the relative contributions of nerves, arteries, and veins for any one of the major cranial foramina in odontocetes, so that it is difficult to infer vascular or neural anatomy for fossils from the form of cranial foramina alone. Comments below focus on the braincase; the face, orbit, and rostrum are not considered.

In extant Cetacea, the main arterial supply to the brain appears to be from a thoracico-spinal rete via spinal meningeal arteries that enter the foramen magnum. The internal carotid artery is small (Fraser and Purves, 1960). In fetal *Physeter catodon* Linnaeus, the internal carotid enters the cranium to participate in the carotid rete mirabile (Melnikov, 1997), but in adult *Physeter catodon, Tursiops truncatus,* and *Monodon monoceros* Linnaeus the vessel is occluded (McFarland et al., 1979; Vogl and Fisher, 1981; Melnikov, 1997). Nonetheless, a patent carotid foramen is a persistent feature in Cetacea. The role of arteries other than the spinal meningeal and internal carotid is not clear; Fraser and Purves (1960:26) noted that, in one injected unnamed odontocete, the middle meningeal artery, a branch of the internal maxillary artery, was involved in intracranial supply.

Cranial drainage in Odontoceti is understood less well. Fraser and Purves (1960) identified the pterygoid vein, supplemented by the internal maxillary and the internal jugular veins, as important in draining the basicranium. Apparently, none of these veins is associated with foramina that might otherwise be used to judge venous size and function. Furthermore, some

vessels that are intracranial in other mammals are extracranial in extant odontocetes (Fraser and Purves, 1960, fig. 13), through movement of the tympanoperiotic away from the braincase. Now-extracranial features in extant species, and presumably in *S. rayi,* include the ventral and dorsal petrosal venous sinuses and the cavernous sinus. There is no petro-occipital canal for the ventral petrosal sinus, and the squamosal and/or parietal occludes the posterior lacerate foramen dorsal to the periotic (e.g., Fraser and Purves, 1960, pls. 13, 19, 26, 28). Of other venous foramina, the mastoid foramen, for the occipital emissary vein, is obscured or lost through change in contribution of the periotic to the braincase wall. The structure of the ethmoid foramen, orbital fissure, and foramen ovale in *S. rayi* are unrevealing about venous drainage.

In non-cetacean mammals, the most notable foramen that has a venous function alone is probably the postglenoid foramen (also known as the retroarticular, retroglenoid, temporal, or spurious jugular foramen). This lies at the ventral opening of the temporal canal, for passage of the temporal sinus (or dorsal cerebral vein) from the transverse sinus (Sisson and Grossman, 1953; Whitmore, 1953; Padget, 1957, pl. 6; Evans, 1993). In non-cetacean mammals, including Artiodactyla (the presumed sister group to Cetacea), the temporal canal lies wholly within the squamosal. A comparable foramen is absent in Odontoceti and Mysticeti, suggesting that the temporal sinus is lost. It could be claimed that the pathway that Fordyce (1994) identified in *W. maerewhenua* (and, here, in *S. rayi*) as that for the middle meningeal artery actually represents the path of the temporal sinus and, thus, the temporal canal and postglenoid foramen, but this seems unlikely. First, in archaeocetes, a vestigial (non-patent) postglenoid foramen lies at the base of the postglenoid process on the squamosal, posterolateral to the well-developed foramen between the periotic and squamosal that is inferred to mark the path for the middle meningeal artery. Second, the temporal canal in non-cetacean mammals lies within the squamosal, whereas the pathway for the presumed middle meningeal artery in *W. maerewhenua* is a groove on the ventromedial surface of the squamosal, dorsal and lateral to the periotic and associated with a small subcircular fossa (Fordyce, 1994).

Some features of *S. rayi* are similar to those of *W. maerewhenua.* A prominent foramen opens between the squamosal and the lateral wall of the periotic at the fovea epitubaria. More internally (cranially), a foramen, presumably for the middle meningeal artery, lies at the posterior of the parietal-alisphenoid suture near the apex of the anterior process of the periotic; this foramen is presumed to be the homolog of the subcircular fossa as seen in Squalodelphinidae and, as a small cavity, in *W. maerewhenua.* Muizon (1994:137) discussed the broader significance of the subcircular fossa in Platanistoidea, identifying it as present in the squamosal of some species of Squalodontidae, but that homology is questionable. In one well-preserved specimen referred to *Squalodon calvertensis* Kellogg (USNM 23537), a large foramen is present in the ventral surface of the squamosal dorsal to the periotic, but it is directed dorsally into the squamosal; it is not associated with sutures with adjacent bones, and it lacks an associated groove leading toward the foramen ovale. Such a situation contrasts with the combination of foramen (foramen spinosum) and fissure (path for presumed middle meningeal artery, associated with the parietal-alisphenoid-squamosal) that runs toward the foramen ovale from above the periotic in *Waipatia* (Waipatiidae) and from the subcircular fossa above the periotic in *Notocetus* (Squalodelphinidae) and *Zarhachis* (Platanistidae). In *Platanista,* the foramen opens in the squamosal lateral to the periotic, which is visible in ventral view. The feature in *S. calvertensis* thus is probably not related to the subcircular fossa; it could be a nutrient foramen for the squamosal, or it may indicate venous drainage of the posterior of the temporal fossa. Because of its position dorsal to the periotic, it is unlikely that this is the temporal canal. Comparable foramina occur sporadically in other odontocetes, but their taxonomic patterns and function are uncertain.

Other basicranial foramina on odontocete skulls also are problematic. Kellogg (1925) noted small foramina in the basicranium of *Zarhachis flagellator* (Cope), and possibly homologous foramina occur in *W. maerewhenua* (see Fordyce, 1994, fig. 8, foramina 1 and 2). Ridewood (1922) named the squamosal cleft in some mysticetes, where it is a deep fissure that extends ventrally from the temporal fossa to a point on the squamosal opposite the periotic. Comparable features in some extant odontocetes (Monodontidae) are associated with the squamosal/parietal suture in the temporal fossa and may indicate venous drainage; such a pathway is not seen in *S. rayi.*

Phylogenetic Relationships

CLADISTIC ANALYSIS.—*Simocetus rayi* shows derived structures representative of the Odontoceti, and it is not an archaeocete or a mysticete. Further, the overall primitive condition of many features in *S. rayi* suggests a basal position in the clade Odontoceti. Traditionally, basal odontocetes are placed in the family Agorophiidae, a group reviewed below. Archaic form in an organism, however, does not rule out relationships with a more-crownward taxon, and with this in mind extensive point-by-point comparisons of *S. rayi* were made with representatives of all other major odontocete clades. No single features or, notably, structural complexes, were identified that placed *S. rayi* convincingly close to one or more of the Physeteroidea, Ziphiidae, Delphinida, Eurhinodelphinidae, or Platanistoidea. A few ambiguous similarities between *S. rayi* and some of the latter taxa (e.g., toothless premaxilla, elongate conical pterygoid hamulus) are of uncertain value in placing *Simocetus* (see below).

To explore relationships further, *S. rayi* was included in computer-assisted cladistic analyses of odontocetes, which used the taxa, characters, and matrix of Fordyce (1994) as a starting point and added the few derived features (such as toothless premaxilla, elongate conical pterygoid hamulus, and persistent in-

terparietal) that *S. rayi* shares with some more-crownward odontocetes. (Although comparisons are needed with other archaic "agorophiid" odontocetes, none of the latter provide enough information to warrant their inclusion in a cladistic analysis; see below.) In all analyses, *S. rayi* plotted consistently toward the base of the Odontoceti. On the cladogram of Fordyce (1994, fig. 15), it plotted immediately crownward from *Archaeodelphis patrius* but stemward from representative Physeteroidea, Ziphiidae, Delphinida, Eurhinodelphinidae, and Platanistoidea. Figure 18 summarizes the latter relationships. Other than positioning *S. rayi* toward the base of the odontocetes, the cladistic analyses added no new information about patterns among more-crownward odontocetes. For this reason, the characters, procedures, and results offered by Fordyce (1994) are not presented again herein, and the cladistic analysis is not taken any further.

As mentioned above, archaic odontocetes comparable with *Simocetus* previously have been put in the widely debated family Agorophiidae. On this point, several issues immediately require attention. Should the Agorophiidae be used as a clade based upon *Agorophius pygmaeus,* as Fordyce (1981) suggested? Or should Agorophiidae be used more broadly (e.g., Whitmore and Sanders, 1977) as a grade, forming a paraphyletic and perhaps polyphyletic receptacle for enigmatic archaic odontocetes? The latter seems undesirable, although *S. rayi* is still compared below with other described "agorophiid" odontocetes.

On broader relationships, some authors have suggested that the family Agorophiidae belongs with the Squalodontidae in a superfamily Squalodontoidea and, further, that the Squalodontidae may be a near-basal group of odontocetes whence some living groups evolved (e.g., Abel, 1913:221; Simpson, 1945; Slijper, 1979, fig. 36). Rothausen (1968) recognized the desirability of a cladistic approach to the Squalodontidae, and Muizon (1987, 1988a, 1988b, 1991, 1994) later convincingly argued that squalodontids are related closely to *Platanista* and other Platanistoidea. The conclusion herein follows Muizon (and also Fordyce, 1994), and Squalodontoidea is regarded as a synonym of Platanistoidea. There is no reason to think that *S. rayi* is related closely to Squalodontidae. Relationships between *A. pygmaeus* and Squalodontidae have yet to be resolved.

Finally, despite the basal position of *Simocetus rayi,* the species does have a few highly specialized features of the feeding apparatus. These features preclude *S. rayi* from being ancestral to any other described species and indicate that it was an early side branch in odontocete history. For such reasons the species is placed in a new family. All these points are elaborated below.

Simocetus AS AN ODONTOCETE.—*Simocetus rayi* shows a range of features unique to odontocetes, including a posteriorly telescoped supraorbital (ascending) process of the maxilla that is broadened laterally behind the level of the antorbital notch, a posteriorly placed dorsal infraorbital (maxillary) foramen, and the presence of a premaxillary sac fossa, premaxillary sulci,

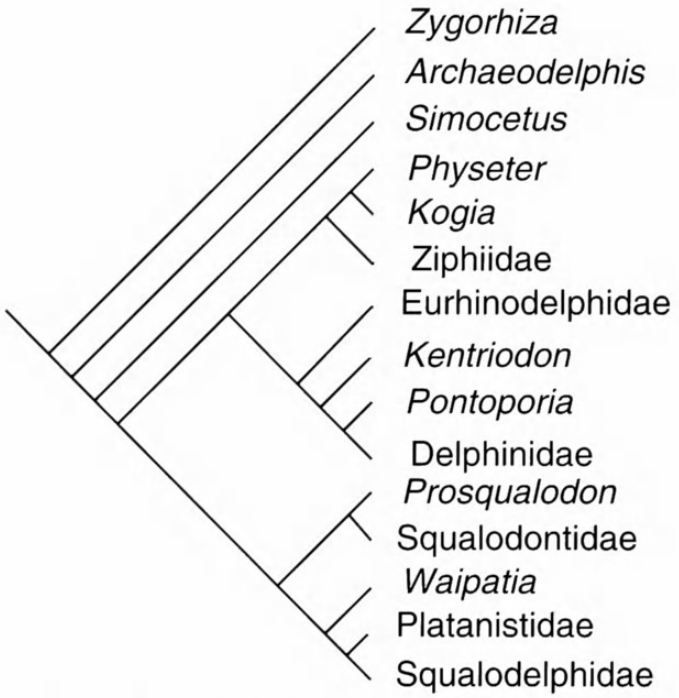

FIGURE 18.—Cladogram showing inferred relationship of *Simocetus rayi* to other major groups of Odontoceti. (†= extinct taxa.)

and premaxillary foramen (or foramina). In the orbit, the infraorbital process of the maxilla is greatly reduced, rather than conspicuous (archaeocetes) or large and plate-like (mysticetes). At the posterior of the face, the orbitotemporal crest is displaced posterodorsally relative to the postorbital ridge, so that the posterior of the face partly roofs the temporal fossa. In contrast, the orbitotemporal crest in archaeocetes (and in the odontocete family Physeteridae) lies immediately dorsal to the postorbital ridge, whereas in mysticetes the orbitotemporal crest is lost or migrates anterodorsally. The distinct antorbital notch forms a vertical groove that faces anteriorly to anterolaterally; this grooved notch is probably a concomitant of the facial fossa developed above the orbit (see comparisons with the archaic odontocetes *Archaeodelphis* and *Xenorophus*, below). An ossified mesethmoid lies between the bony nares. In the basicranium, the parietal lies dorsomedial to the periotic to occlude the cranial hiatus, and the squamosal is presumed to lie above the periotic. Finally, the region of the mandibular foramen is relatively large and ventrally inflated.

SIMILARITIES WITH MYSTICETI.—Odontocetes and mysticetes do share features not seen in archaeocetes, pointing to their sister-group relationship. Some of these features are conspicuous in *S. rayi.* For example, a cluster of dorsal infraorbital foramina opens at the base of the rostrum in *S. rayi* and in the archaic mysticete *Mammalodon colliveri.* The mesorostral groove in *S. rayi* and mysticetes is well developed anteriorly on the rostrum, but there is no anterior groove in archaeocetes; rather, the premaxillae contact each other here at a planar median suture. *Simocetus rayi,* other odontocetes, and Mysticeti are amastoid, with the posterior (mastoid) process of the peri-

otic not exposed laterally on the skull wall. This may be linked with the reduced or lost contact between the periotic and exoccipital, which, in turn, perhaps reflects the development of the peribullary sinus. Teeth in odontocetes and toothed mysticetes lie anterior to the antorbital notch, but in all described odontocetes they are farther forward than in archaic mysticetes of the genus *Aetiocetus* (see Barnes et al., 1995). The short mandibular symphysis in *S. rayi* is reminiscent of that seen in mysticetes, but the structure in *S. rayi* is more extensive anteroposteriorly. As in mysticetes, there is an indistinct longitudinal groove toward the ventral surface of the symphysis, but whether the groove is homoplasious or synapomorphic is uncertain. The large mandibular foramen and its associated thin lateral wall ("panbone") are similar between odontocetes and archaic mysticetes, apart from the ventral inflation seen in odontocetes. Comparable structures occur in basilosaurid archaeocetes; more study of homology and function is needed.

CURRENT CONCEPTS AND PROBLEMS OF ODONTOCETE PHYLOGENY.—Recent cladistic analyses by Muizon (1987, 1988a, 1988b, 1991), Heyning (1989, 1997), Barnes (1990), and Fordyce (1994) help to elucidate family-level patterns within the Odontoceti and help to interpret the relationships of *S. rayi*. Sperm whales, Physeteroidea (Physeteridae and Kogiidae), are odontocetes (cf. Milinkovitch, 1995) that form a sister group to Ziphiidae. Physeteroidea and Ziphiidae together represent the Physeterida (see Muizon, 1991; Fordyce, 1994). Alternatively, sperm whales may constitute a sister group to all other odontocetes (Heyning, 1989, 1997; Barnes, 1990). The Platanistoidea (sensu Muizon, 1987, 1991; Fordyce 1994) encompasses Platanistidae, Squalodelphinidae, Waipatiidae, Squalodontidae, and perhaps Dalpiazinidae. Delphinida (sensu Muizon, 1988b) includes the Delphinoidea (Delphinidae, Phocoenidae, Monodontidae, Albireonidae, and Kentriodontidae) along with some of the "river dolphins" (Iniidae, Pontoporiidae, and the uncertainly distinct Lipotidae). Less clear are the relationships of Eurhinodelphinidae and Eoplatanistidae, which Muizon (1991) included in Eurhinodelphinoidea, a sister group to Delphinida.

Despite recent efforts, the cladistic relationships between the major groups Physeteroidea, Ziphiidae, Delphinida, Eurhinodelphinoidea, and Platanistoidea seem weakly resolved. Characters cited by Muizon and Barnes in support of their cladograms are debatable in terms of distribution among taxa (homoplasy was not always identified), applicability (a state was not always seen in all members of a clade), and polarity (the primitive versus derived states were not always clear, and transition series were not always clear-cut). Fordyce (1994) attempted to circumvent such problems through a computer analysis of an explicit matrix of characters, but even then (Fordyce, 1994, fig. 15) some of the key nodes among the Odontoceti were supported by rather few characters including reversals and features of debatable polarity (e.g., ossified lateral lamina of pterygoid sinus fossa). Heyning (1989, without data matrix; 1997, with data presented) considered only extant odontocetes, yet fossils in general are known to influence cladograms profoundly (Donoghue et al., 1989). Is there hope to get beyond this situation by using traditional anatomy, as opposed to molecular phylogeny? The described species of odontocetes, fossil and recent, have been studied in such detail and for so long that it is difficult to imagine new insights into higher relationships arising from more studies of described material. Rather, new discoveries of well-preserved fossil skulls will more likely provide the key. This is particularly the case for Oligocene fossils; material in the largely unstudied Emlong collection offers great promise.

FAMILY AGOROPHIIDAE.—The Family Agorophiidae has long been considered to encompass the phylogenetically and geologically oldest odontocetes. Supposed diagnostic features of the family (e.g., Kellogg, 1923b, and other references reviewed by Fordyce, 1981) include the presence of heterodont teeth and a primitively telescoped skull with a large intertemporal constriction. Such features occur in *Simocetus,* which might, therefore, be viewed as an agorophiid. These supposed diagnostic features of agorophiids, however, are plesiomorphies of no value in assessing immediate relationships. To judge the relationship between *Simocetus* and Agorophiidae, the latter family first should be rediagnosed on the basis of derived characters. Any rediagnosis must be based initially upon *Agorophius pygmaeus* (Müller, 1849), which is the type species and only species in the genus *Agorophius* Cope, 1895, and in turn is the type genus of the family Agorophiidae Abel, 1913.

Agorophius pygmaeus is known with certainty only from the holotype skull, from the Cooper Marl (Chattian, late Oligocene) of South Carolina (Whitmore and Sanders, 1977). No other described fossils undoubtedly belong to this species or in *Agorophius,* although Albert E. Sanders recently collected an apparently conspecific skull. One species possibly close to *A. pygmaeus* is "*Squalodon* (*Microzeuglodon*?)" *wingei* Ravn, 1926, the hypodigm of which consists of teeth, a bulla, and undescribed skull fragments from the upper Oligocene of Denmark. (Rothausen (1970) indicated that this species does not belong to *Squalodon,* and used the new generic name "*Oligosqualodon,*" a nomen nudum, for the species.) Like *A. pygmaeus,* "*Squalodon* (*Microzeuglodon*?)" *wingei* has a cheek tooth with a high crown, indistinctly elevated denticles, and limited ornament. Relationships between these species could be elucidated if other topotypic material is found.

The holotype skull of *A. pygmaeus* is lost, and only a cheek tooth remains (specimen MCZ 8761; Fordyce, 1981), but some details of the lost skull appear in a lithograph (True, 1907, pl. 6). Clearly, *Agorophius pygmaeus* is an archaic odontocete. The lithograph shows overall profiles and some sutures and foramina; the skull has a prominent supraorbital process of the maxilla, a marked intertemporal constriction, a robust zygomatic process, and a moderately large, denticulate, smooth, high-crowned cheek tooth. The basicranium, tympanoperiotic, most teeth, and the mandible appear to be missing, however, and few or no details can be seen for the supraorbital process of

the maxilla, dorsal infraorbital foramen, premaxillary sac fossa and sulci, anterior of rostrum, antorbital notch, lacrimal, nasals, orbit, and palate. Overall, the lithograph seems good enough to judge whether any new topotypic fossils might be conspecific with the lost holotype skull, and it allows limited comparisons with *S. rayi* and other archaic odontocetes. It appears, however, not to provide enough information to allow the Agorophiidae to be rediagnosed in a cladistic sense. Should we then maintain a grade family Agorophiidae for archaic odontocetes such as *Xenorophus sloani, Archaeodelphis patrius,* and *Simocetus rayi*? Perhaps not; although grade families offer easy classification of incomplete specimens, and limit the numbers of monotypic high-level basal clades, they also obscure relationships and thus oversimplify phylogenetic history. For now, the broad traditional use of Agorophiidae is not followed, and the family is used herein only for *A. pygmaeus*.

Beyond *Agorophius pygmaeus,* odontocetes previously referred to the Agorophiidae include *Archaeodelphis patrius* Allen (1921), *Atropatenocetus posteocenicus* Aslanova (1977), *Microzeuglodon caucasicum* (Lydekker, 1893), *Mirocetus riabinini* Mchedlidze (1970), and *Xenorophus sloani* Kellogg (1923b). Kellogg (1923a), Simpson (1945), Whitmore and Sanders (1977), Barnes (1978), and Fordyce (1981), among others, have commented on the family placement of these species. Comparisons with all, below, are based largely upon published accounts.

COMPARISONS OF *Simocetus* AND *Agorophius*.—Conspicuous primitive (plesiomorphic) features on the skull of *S. rayi* provide superficial similarity with *A. pygmaeus,* and, indeed, Muizon (1991:303) identified USNM 256517 (the holotype of *S. rayi*) as belonging in *Agorophius*. Shared primitive features include a facial fossa that is only moderately developed, a large temporal fossa open to dorsal view rather than roofed by adjacent bones, an intertemporal constriction with the parietals exposed dorsally, prominent nuchal crests, and heterodont teeth. (*S. rayi* does show other plesiomorphies, such as the broadly exposed palatine and a pterygoid sinus fossa that is restricted to the basicranium, but comparable features cannot be seen in *A. pygmaeus*.)

More importantly, *S. rayi* is more derived than *A. pygmaeus* in some features. Its rostrum is quite dorsoventrally compressed and anteriorly deflected, with a transversely convex ventral surface, whereas that of *A. pygmaeus* appears to be straight. The braincase is more inflated at the base of the zygomatic process, and there is a deep cleft between the zygomatic process and the braincase. The outline of the supraoccipital is more hemispherical (dorsal view), the postglenoid process is thicker (lateral view), and the exoccipital extends farther laterally. Notably, *Agorophius pygmaeus* is more derived than *S. rayi* in its more laterally expanded supraorbital process of the maxilla and greater number of maxillary teeth (eight or more).

Comparisons of teeth also reveal differences, although it is not easy to judge their taxonomic significance. Mandibular cheek teeth in *S. rayi* differ from the one upper middle cheek tooth of *A. pygmaeus* in the (presumably) derived states of smaller absolute size, relatively lower crowns, relatively smaller main denticle and more free-standing accessory denticles, and more transversely compressed crowns. In *S. rayi,* also, tooth crowns are more asymmetrical (lateral view) and ornamented, with the main denticles displaced relatively anteriorly, but whether these conditions are primitive or derived is uncertain.

In summary, the plesiomorphies seen in these two species do not demonstrate close relationships. Furthermore, each species shows specialized features that seem to rule out close relationships. For this reason, *S.* rayi is excluded from the Agorophiidae. Differences with other archaic odontocetes, elaborated below, reinforce the suggestion that *S. rayi* belongs in its own family Simocetidae.

COMPARISONS OF *Simocetus* AND *Archaeodelphis*.—The enigmatic, monotypic small species *Archaeodelphis patrius* Allen, 1921, is perhaps the most archaic odontocete described. Whitmore and Sanders (1977:305) assigned it to the Cetacea incertae sedis, whereas Fordyce (1994, fig. 15) placed it at the base of the Odontoceti. Its age is possibly Oligocene (Whitmore and Sanders, 1977).

Brief examination of the holotype and only specimen of *A. patrius* (MCZ 15749; skull lacking rostrum and bullae) revealed notable differences from *S. rayi. Simocetus rayi* is more derived in having facial structures more posteriorly displaced (facial fossa, supraorbital process of the maxilla, an ascending process of the premaxilla, and dorsal maxillary foramina), a posteriorly bifurcated premaxilla, a more elevated lateral margin of the rostrum, the relatively shorter nasals, a relatively longer and more delicate postorbital process of the frontal, a robust and transversely thickened zygomatic process of the squamosal, larger pterygoid sinus fossae, long, medially apposed pterygoid hamuli into which the pterygoid sinuses extend, a more prominent basioccipital crest, a more anteroposteriorly thickened postglenoid process, and a more posterodorsally displayed orbitotemporal crest on the frontal.

Despite its overall archaic form, *Archaeodelphis patrius* seems quite specialized in its relatively large lacrimal, deep medial cleft between the palatines posteriorly, and thick, platelike extensions of the medial lamina of the pterygoid that meet medially to roof the choanae. As in most other odontocetes (cf. *S. rayi*), the foramen ovale is not confluent with the posterior lacerate foramen. The structure of the medial lamina of the pterygoid is so unusual that, despite its archaic structure, *A. patrius* is probably not ancestral to any other known odontocete, although perhaps the enlarged lacrimal indicates affinity with *Xenorophus sloani*. There is no evidence to support a close relationship with *S. rayi*.

COMPARISONS OF *Simocetus* AND *Xenorophus*.—The late Oligocene species *Xenorophus sloani* Kellogg (1923b) is known from the holotype (USNM 11049), an incomplete skull that lacks the tip of the rostrum, the region around the premaxillary sac fossa, and the braincase posterior to the orbits. Other

specimens referable to *Xenorophus* were mentioned and figured by Whitmore and Sanders (1977), but they have not been described formally. Comparisons below are based upon study of the holotype skull and upon published illustrations (Miller, 1923, pl. 5: fig. 6; Whitmore and Sanders, 1977, fig. 1a).

There are major differences between *S. rayi* and *X. sloani*. As with *A. patrius, S. rayi* is more derived in its posteriorly displaced facial structures (facial fossa, supraorbital process of the maxilla, ascending process of the premaxilla, and posterodorsally oriented dorsal maxillary foramina), posteriorly bifurcated premaxilla, and more elevated lateral margin of the rostrum (resulting in a less abruptly elevated orbit). The antorbital notch is more prominent (dorsoventrally more shallow, anteroposteriorly deeper), the premaxillary sac fossa is broader and more tabular (although the premaxilla in *X. sloani* is broken, a narrow long fossa is indicated), the premaxillary sulci are more prominent, and the anterior of the mesorostral groove is more open. The cheek teeth are relatively smaller, more transversely compressed, and more emergent from the alveoli, and they have large diastemata. The palate is ventrally convex rather than flat in transverse profile and the anterior of the rostrum is dorsoventrally thin and deflected ventrally (what remains in *X. sloani* does not indicate deflection). The rostrum is relatively shorter, wider, and less abruptly attenuated, and ventrally, the posterior of the palate is relatively wider and less abruptly attenuated. The postorbital process of the frontal is relatively longer and more delicate, and the intertemporal area is shorter and wider. Finally, the supraoccipital is produced more anteriorly.

Despite its generally archaic form, *Xenorophus sloani* shows some intriguing derived features. A very large lacrimal dominates the preorbital and supraorbital parts of the cranium, and the supraorbital process of the maxilla is large and produced far posteriorly. Also notable are the prominent prenarial constriction, nares that open well behind the level of the antorbital notch, multiple cheek teeth with a triangular low crown and multiple small denticles, and a relatively short exposure of the frontals on the vertex. Lacrimal size alone seems to rule out affinities with any more-crownward odontocete, and there is no evidence to support a close relationship with *S. rayi*.

COMPARISONS OF *Simocetus* AND *Atropatenocetus*.—*Atropatenocetus posteocenicus* Aslanova, 1977, was described as a new genus and species of Agorophiidae. The holotype and only described specimen is a quite incomplete skull with fragmentary mandibles presumably from the upper Oligocene of Apsheron Peninsula, Azerbaijan. The supraorbital process of the maxilla appears to be displaced posterodorsally over the frontal. The cheek teeth are relatively larger and lower crowned than *S. rayi,* and they possess papillate ornament on the cingula. Otherwise, more meaningful comparisons are difficult. There is no hint of features that would place this species close to *Simocetus rayi* or, for that matter, *Agorophius pygmaeus*.

COMPARISONS OF *Simocetus* AND *Microzeuglodon*.—*Microzeuglodon caucasicum* (Lydekker, 1893) is known only from the holotype: a posterior fragment of the left mandible with four cheek teeth, an unfigured second fragment of the jaw with five broken teeth, a left humerus, and an incomplete caudal vertebra, from an uncertain horizon in the Oligocene of Azerbaijan (Kellogg, 1923a; Mchedlidze, 1964). The species has been discussed widely without consensus as to its affinities. The large size of the mandible and teeth, relatively high crowns, prominent lingual cingula and level of insertion of the teeth, and relatively narrow diastemata suggest that *M. caucasicum* is not related closely to *S. rayi*.

COMPARISONS OF *Simocetus* AND *Mirocetus*.—*Mirocetus riabinini* Mchedlidze, 1970, is known only from the holotype skull and associated partial postcranial skeleton from the upper Oligocene of Caucasus. (Initially, Riabinin (1938) identified the holotype as *Microzeuglodon* aff. *caucasicus*.) The skull is distorted, albeit with basic topography preserved (Riabinin, 1938), but sutural details are unclear (K. Rothausen, pers. comm., 1980). Of note, the skull appears to possess posteriorly displaced facial fossae, which suggests that *M. riabinini* is an odontocete, rather than a species of Aetiocetidae (cf. Mchedlidze, 1976). Some features in *M. riabinini* suggest at least that it is not conspecific with *S. rayi;* for example, the skull and teeth are notably larger, the rostrum is more narrow (plesiomorphy), the supraorbital process extends farther laterally, the postorbital process is robust with a widened apex, a sagittal crest appears to be present (plesiomorphy), the zygomatic process is relatively shorter and possesses a more recurved ventral surface (plesiomorphy), the braincase is not markedly inflated anteroexternally, the supraoccipital apex is sharp, and the teeth are not inserted at the lateral edge of the rostrum. *Mirocetus riabinini* is similar to *S. rayi* in that the cheek teeth appear to be emergent, with parallel roots united by an isthmus, and diastemata are prominent. No features clearly indicate close relationship between *M. riabinini* and *S. rayi* or, for that matter, *A. pygmaeus*.

COMPARISONS WITH OTHER HETERODONT ODONTOCETES.—Other named species of heterodont odontocetes might be compared with *S. rayi*. Among these are many so-called Squalodontidae based upon isolated teeth; examples from the middle Tertiary of the North American Atlantic Coastal Plain include "*Phoca*" *debilis,* "*Phoca*" *modesta, Colophonodon holmesii*, and "*Squalodon*" *protervus*. Arguably, such names based upon isolated teeth are nomina dubia, although it is always possible that such teeth will be found in place in topotypic skulls, which, in turn, might elucidate relationships. For now, these taxa cannot be compared usefully with *S. rayi*.

RELATIONSHIPS WITH OTHER GROUPS OF ODONTOCETES.—A few other comparisons warrant attention. Although *S. rayi* is dramatically different from Eurhinodelphinidae in overall skull form, it is similar to some eurhinodelphinids in having a toothless premaxilla, an elongate conical pterygoid hamulus, a thick postglenoid process, and a recurved anteroexternal sulcus on the periotic. In all species of *Eurhinodelphis* (e.g., *E. bossi* Kellogg, 1925), the toothless premaxillae are elongate, forming

a tapered distal part to the rostrum similar to that of longirostral teleosts, and in marked contrast to the short flattened distal toothless premaxillae of *S. rayi*. *Simocetus rayi* has elongate conical pterygoid hamuli, similar to those of *Argyrocetus joaquinensis* (figured in Kellogg, 1932). Elongate subcylindrical hamuli also occur in an unnamed archaic odontocete USNM 243979 (the so-called non-squalodontid odontocete of Whitmore and Sanders, 1977, fig. 2a, from ?Pysht Formation, Washington) that is not demonstrably a eurhinodelphinid. Hamular structure is known too poorly among basal odontocetes to allow reliable use in higher taxonomy. The postglenoid process in *S. rayi* is anteroposteriorly thick, as seen also in species of *Eurhinodelphis* (e.g., Kellogg, 1925). A thick postglenoid process, however, also occurs in the enigmatic *Squaloziphius emlongi* Muizon, 1991 (a possible eurhinodelphinid), and in some ziphiids; the functional significance of such thickening is uncertain. On the periotic, the ventral part of the anteroexternal sulcus is recurved forward, as seen in some eurhinodelphinids (Fordyce, 1983b), but the sulcus is shallow and indistinct in contrast to the deep sulcus of eurhinodelphinids. In this respect, the anteroexternal sulcus is more similar to that of the platanistoid groups *Waipatia* and Squalodelphinidae. For now, eurhinodelphinid relationships cannot be ruled out, but they are not supported strongly.

Simocetus rayi is similar to some extant Delphinidae (such as *Orcaella brevirostris* (Owen)) in having an identifiable or incompletely sutured interparietal in the adult. Sutures between the interparietal and adjacent elements sometimes persist in adults of other species of delphinid. This condition may be interpreted as paedomorphic. An interparietal is distinct also in late fetal stages of some mysticetes (Ridewood, 1922). Many delphinids, as with *S. rayi,* also have a short unfused mandibular symphysis. Some delphinids (e.g., *Grampus griseus*) also have a palate with scattered multiple small palatine foramina, although this condition also is seen in Squalodontidae. Such features might indicate a relationship with Delphinidae or other Delphinoidea, but more convincing similarities (involving, e.g., the pterygoid sinus complex, premaxillae, and periotic) are lacking.

As with the platanistoids *Waipatia maerewhenua* and Squalodelphinidae, *S. rayi* has a pronounced cleft—associated with or representing the foramen spinosum, and thus presumably for the middle meningeal artery—arising near the foramen ovale and trending posterolaterally toward the periotic along or near the parieto-squamosal suture. Even in the rather archaic *W. maerewhenua,* however, the foramen spinosum lies dorsal to and is obscured by the periotic, and the foramen in Squalodelphinidae is transformed into a large subcircular fossa, whereas in *S. rayi* a foramen opens medial to the periotic and is clearly visible in ventral view. The condition in *S. rayi* could be interpreted as trending toward that of some platanistoids. Similar forms of the anteroexternal sulcus of the periotic were noted above. Beyond these, there is little particular support for platanistoid relationships.

Summary

Morphological comparisons do not clearly indicate relationships. This was emphasized during cladistic analyses, when, despite the above similarities, *S. rayi* did not cluster with any particular more-crownward clade. A more-crownward position might have been forced by character weighting, or by invoking an ordered transition series for some supposed key characters, or by invoking accelerated character transformation, but such techniques seem inappropriate given the poor understanding of the anatomy of archaic odontocetes.

Superimposed on the archaic skull of this peculiar ancient taxon are some features that are, unexpectedly, highly specialized: the premaxilla is toothless and dorsoventrally flattened, the rostrum is relatively short and broad, and the anterior of the rostrum and mandible are markedly downturned. Such attributes indicate specialized feeding behavior. Other unusual features are plausibly but less clearly autapomorphies; these include the nonpolydont tooth complement (primitive, or secondarily reduced from polydont state?), broad diastemata between posterior cheek teeth, narrow rather than laterally expanded supraorbital process of the maxilla (again, primitive, or secondarily reduced from a broader state?), and the mediolaterally deep optic infundibulum. Previously published literature might give the impression that archaic odontocetes—"agorophiids"—are primitive overall, but *Simocetus* demonstrates that archaic taxa may indeed represent specialized side branches in odontocete history that are not close to modern clades. *Simocetus rayi* nevertheless shows the distinctive facial structure seen in most other odontocetes, emphasizing the early development—presumably in the most archaic of the odontocetes—of the nasofacial soft tissues and probably of echolocation abilities.

Literature Cited

Abel, O.
1913. Die Vorfahren der Bartenwale. *Denkschriften der Akademie der Wissenschaften, Wien, Mathematisch-Naturwissenschaftliche Klasse,* 90:155–224, 12 plates.

Allen, G.M.
1921. A New Fossil Cetacean (*Archaeodelphis patrius* gen. et sp. nov.). *Bulletin of the Museum of Comparative Zoology at Harvard College,* 65:1–14.

Aslanova, S.M.
1977. [A New Genus of Cetaceans (*Atropatenocetus posteocenicus* gen. et sp. nov.) from the Oligocene of Azerbaijan.] *Doklady Akademia Nauk Azerbaidzhanskoi SSR,* 33:60–64. [In Russian.]

Barnes, L.G.
1978. A Review of *Lophocetus* and *Liolithax* and Their Relationships to the Delphinoid Family Kentriodontidae (Cetacea: Odontoceti). *Science Bulletin of the Natural History Museum of Los Angeles County,* 28:1–35.
1990. The Fossil Record and Evolutionary Relationships of the Genus *Tursiops*. *In* S. Leatherwood and R.R. Reeves, editors, *The Bottlenose Dolphin,* pages 3–26. San Diego: Academic Press.

Barnes, L.G., M. Kimura, H. Furusawa, and H. Sawamura
1995. Classification and Distribution of Oligocene Aetiocetidae (Cetacea; Mysticeti) from Western North America and Japan. *The Island Arc,* 3(4):392–431.

Boenninghaus, G.
1904. Das Ohr des Zahnwales. *Zoologische Jahrbücher, Abteilung für Anatomie und Ontogenie der Tiere,* 19:189–360.

Breathnach, A.S.
1960. The Cetacean Nervous System. *Biological Review,* 35:187–230.

Brownell, R.L., and E.S. Herald
1972. *Lipotes vexillifer. Mammalian Species,* 10: 4 pages.

Cope, E.D.
1895. Fourth Contribution to the Marine Fauna of the Miocene Period of the United States. *Proceedings of the American Philosophical Society,* 34:135–155.

Cranford, T.W., M. Amundin, and K.S. Norris
1996. Functional Morphology and Homology in the Odontocete Nasal Complex: Implications for Sound Generation. *Journal of Morphology,* 228:223–285.

Curry, B.E.
1992. Facial Anatomy and Potential Function of Facial Structures for Sound Production in the Harbor Porpoise (*Phocoena phocoena*) and Dall's Porpoise (*Phocoenoides dalli*). *Canadian Journal of Zoology,* 70:2103–2114.

Dart, R.A.
1923. The Brain of the Zeuglodontidae (Cetacea). *Proceedings of the Zoological Society of London,* 1923:615–648.

Davis, D.D.
1964. The Giant Panda: A Morphological Study of Evolutionary Mechanisms. *Fieldiana, Zoology Memoirs,* 3:1–339.

Domning, D.P.
1978. Sirenian Evolution in the North Pacific. *University of California Publications in Geological Sciences,* 118:1–176.

Domning, D.P., C.E. Ray, and M.C. McKenna
1986. Two New Oligocene Desmostylians and a Discussion of Tethytherian Systematics. *Smithsonian Contributions to Paleobiology,* 59: 1–56.

Donoghue, M.J., J.A. Doyle, J. Gauthier, A.G. Kluge, and T. Rowe
1989. The Importance of Fossils in Phylogeny Reconstruction. *Annual Reviews of Ecology and Systematics,* 20:431–460.

Edinger, T.
1955. Hearing and Smell in Cetacean History. *Monatschrift für Psychiatrie und Neurologie,* 129:37–58.

Evans, H.E., editor
1993. *Miller's Anatomy of the Dog.* Third edition, 1113 pages. Philadelphia: W.B. Saunders.

Flynn, T.T.
1948. Description of *Prosqualodon davidi* Flynn, a Fossil Cetacean from Tasmania. *Transactions of the Zoological Society of London,* 25: 153–197.

Fordyce, R.E.
1981. Systematics of the Odontocete *Agorophius pygmaeus* and the Family Agorophiidae (Mammalia: Cetacea). *Journal of Paleontology,* 55:1028–1045.
1983a. Dental Anomaly in a Fossil Squalodont Dolphin from New Zealand, and the Evolution of Polydonty in Whales. *New Zealand Journal of Zoology,* 9:419–426.
1983b. Rhabdosteid Dolphins (Mammalia: Cetacea) from the Middle Miocene, Lake Frome Area, South Australia. *Alcheringa,* 7:27–40.
1994. *Waipatia maerewhenua,* New Genus and New Species (Waipatiidae, New Family), an Archaic Late Oligocene Dolphin (Cetacea: Odontoceti: Platanistoidea) from New Zealand. *Proceedings of the San Diego Museum of Natural History,* 29:147–176.

Fraser, F.C., and P.E. Purves
1960. Hearing in Cetaceans: Evolution of the Accessory Air Sacs and the Structure of the Outer and Middle Ear in Recent Cetaceans. *Bulletin of the British Museum (Natural History), Zoology,* 7:1–140 pages, frontispiece, plates 1–53.

Heyning, J.E.
1989. Comparative Facial Anatomy of Beaked Whales (Ziphiidae) and a Systematic Revision among the Families of Extant Odontoceti. *Contributions in Science, Natural History Museum of Los Angeles County,* 405:1–64.
1997. Sperm Whale Phylogeny Revisited: Analysis of the Morphological Evidence. *Marine Mammal Science,* 13(4):596–613.

Heyning, J.E., and J.G. Mead
1990. Evolution of the Nasal Anatomy of Cetaceans. *In* J. Thomas and R. Kastelein, editors, *Sensory Abilities of Cetaceans,* pages 67–69. New York: Plenum Press.

Howell, A.B.
1927. Contribution to the Anatomy of the Chinese Finless Porpoise *Neomeris phocaenoides. Proceedings of the United States National Museum,* 70(13): 43 pages [publication 2662].

Huber, E.
1930. Evolution of Facial Musculature and Cutaneous Field of Trigeminus. *Quarterly Review of Biology,* 5:133–187.
1934. Anatomical Notes on Pinnipedia and Cetacea. *Carnegie Institution of Washington Publication,* 447:105–136.

Kasuya, T.
1973. Systematic Consideration of Recent Toothed Whales Based on the Morphology of Tympano-Periotic Bone. *Scientific Reports of the Whales Research Institute, Tokyo,* 25:1–103.

Kellogg, R.
1923a. Description of Two Squalodonts Recently Discovered in the Calvert Cliffs, Maryland; and Notes on the Shark-Toothed Dolphins. *Proceedings of the United States National Museum,* 62(6):1–69.
1923b. Description of an Apparently New Toothed Cetacean from South Carolina. *Smithsonian Miscellaneous Collections,* 76(7): 7 pages, 2 plates.
1925. On the Occurrence of Remains of Fossil Porpoises of the Genus *Eurhinodelphis* in North America. *Proceedings of the United States National Museum,* 66(26):1–40.
1926. Supplementary Observations on the Skull of the Fossil Porpoise *Zarhachis flagellator. Proceedings of the United States National Museum,* 67(28): 18 pages, 5 plates.
1928. History of Whales: Their Adaptation to Life in the Water. *Quarterly Review of Biology,* 3:29–76, 174–208.
1932. A Miocene Long-Beaked Porpoise from California. *Smithsonian Miscellaneous Collections,* 87(2): 11 pages, 4 plates.
1936. A Review of the Archaeoceti. *Carnegie Institution of Washington Publication,* 82: 366 pages, 37 plates.

King, J.E.
1961. The Feeding Mechanism and Jaws of the Crabeater Seal (*Lobodon carcinophagus*). *Mammalia,* 25:462–466.

Lawrence, B., and W.E. Schevill
1956. The Functional Anatomy of the Delphinid Nose. *Bulletin of the Museum of Comparative Zoology at Harvard College,* 114:103–151.

Lydekker, R.
1893. On Zeuglodont and Other Cetacean Remains from the Tertiary of the Caucasus. *Proceedings of the Zoological Society of London,* 1892:558–564.

McFarland, W.L., M.S. Jacobs, and P.J. Morgane
1979. Blood Supply to the Brain of the Dolphin, *Tursiops truncatus*, with Comparative Observations on Special Aspects of the Cerebrovascular Supply of Other Vertebrates. *Neuroscience and Biobehavioural Reviews*, supplement 1, 3:1–93.

Mchedlidze, G.A.
1964. [Fossil Cetaceans of Caucasus.] 144 pages. Tbilisi, Georgia: Izdatel'stvo Metsniereba. [In Russian.]
1970. [Some Features of the Historical Development of the Cetacea, Part 1.] 112 pages. Tbilisi, Georgia : Metsniereba. [In Russian.]
1976. [The Basic Features of the Paleobiological History of the Cetacea.] 136 pages. Tbilisi, Georgia: Metsniereba. [In Russian.]

Mead, J.G.
1975. Anatomy of the External Nasal Passages and Facial Complex in the Delphinidae (Mammalia: Cetacea). *Smithsonian Contributions to Zoology*, 207:1–72.

Melnikov V.V.
1997. The Arterial System of the Sperm Whale (*Physeter macrocephalus*). *Journal of Morphology*, 234(1):37–50.

Milinkovitch, M.C.
1995. Molecular Phylogeny of Cetaceans Prompts Revision of Morphological Transformations. *Trends in Ecology and Evolution*, 10(8): 328–334.

Miller, G.S.
1923. The Telescoping of the Cetacean Skull. *Smithsonian Miscellaneous Collections*, 76(5): 70 pages, 8 plates.

Moris, F.
1969. Étude anatomique de la région céphalique du marsouin *Phocaena phocaena* L. (Cetacé: Odontocete). *Mammalia*, 33:666–726.

Müller, J.
1849. *Über die fossilen Reste der Zeuglodonten von Nordamerica, mit Rucksicht auf die europäischen Reste aus dieser familie*. 38 pages. Berlin: Reimer.

Muizon, C. de
1986. Un nouveau Phocoenidae (Odontoceti, Cetacea) du Miocène supérieur de la Formation Pisco (Pérou). *Comptes Rendus de l'Academie des Sciences*, series 2, 303:1509–1512.
1987. The Affinities of *Notocetus vanbenedeni*, an Early Miocene Platanistoid (Cetacea, Mammalia) from Patagonia, Southern Argentina. *American Museum Novitates*, 2904: 27 pages.
1988a. Le polyphylétisme des Acrodelphidae, Odontocètes longirostres du Miocène européen. *Bulletin du Muséum Nationale d'Histoire Naturelle* (Paris), series 4, section C, 10(1):31–88.
1988b. Les relations phylogénétiques des Delphinida (Cetacea, Mammalia). *Annales de Paléontologie*, 74(4):159–227.
1988c. Les vertébrés fossiles de la Formation Pisco (Pérou), Troisième partie: Les odontocètes (Cetacea, Mammalia) du Miocène. *Mémoires de l'Institut Français d'Études Andines*, 78:1–244.
1991. A New Ziphiidae (Cetacea) from the Early Miocene of Washington State (USA) and Phylogenetic Analysis of the Major Groups of Odontocetes. *Bulletin du Muséum Nationale d'Histoire Naturelle*, Paris, series 4, section C, 12(3–4):279–326.
1994. Are the Squalodonts Related to the Platanistoids? *Proceedings of the San Diego Museum of Natural History*, 29:135–146.

Norris, K.S.
1968. The Evolution of Acoustic Mechanisms in Odontocete Cetaceans. *In* E.T. Drake, editor, *Evolution and Environment*, pages 297–324. New Haven: Yale University Press.

Novacek, M.J.
1986. The Skull of Leptictid Insectivorans and the Higher-Level Classification of Eutherian Mammals. *Bulletin of the American Museum of Natural History*, 183(1):1–112.

Padget, D.H.
1957. The Development of the Cranial Venous System in Man, from the Viewpoint of Comparative Anatomy. *Contributions to Embryology, Carnegie Institution of Washington*, 36:79–140.

Perrin, W.F.
1975. Variation of Spotted and Spinner Porpoise (Genus *Stenella*) in the Eastern Tropical Pacific and Hawaii. *Bulletin of the Scripps Institution of Oceanography*, 21:1–206.

Quay, W.B., and E.D. Mitchell
1971. Structure and Sensory Apparatus of Oral Remnants of the Nasopalatine Canals in the Fin Whale (*Balaenoptera physalus* L.). *Journal of Morphology*, 34:271–280.

Ravn, J.P.J.
1926. On a Cetacean, *Squalodon* (*Microzeuglodon*?) *wingei* nov. sp., from the Oligocene of Jutland. *Meddelelser fra Dansk Geologisk Forening*, 7:45–54.

Ray, C.E.
1976. Fossil Marine Mammals of Oregon. *Systematic Zoology*, 25:420–436. [Date on title page is 1976; actually published in 1977.]
1980. [Obituary] Douglas Ralph Emlong 1942–1980. *News Bulletin of the Society of Vertebrate Paleontology*, 120:45–46.

Riabinin, A.N.
1938. *Microzeuglodon* aff. *caucasicum* Lyd. iz verkne-Maikopskikh otlozhenii Kabristana. *Problemy Paleontologii*, 4:137–185.

Ridewood, W.G.
1922. Observations on the Skull in Foetal Specimens of Whales in the Genera *Megaptera* and *Balaenoptera*. *Philosophical Transactions of the Royal Society of London*, series B, 211:209–272.

Rothausen, K.
1968. Die systematische Stellung der europäischen Squalodontidae (Odontoceti: Mamm.). *Paläontologische Zeitschrift*, 42:83–104.
1971. Marine Reptilia and Mammalia and the Problem of the Oligocene-Miocene Boundary. *Giornale di Geologia*, series 2, 35:181–189.

Schenkkan, E.J.
1973. On the Comparative Anatomy and Function of the Nasal Tract in Odontocetes (Mammalia, Cetacea). *Bijdragen Tot de Dierkunde*, 43:127–159.

Schenkkan, E.J., and P.E. Purves
1973. The Comparative Anatomy of the Nasal Tract and the Function of the Spermaceti Organ in the Physeteridae (Mammalia, Odontoceti). *Bijdragen Tot de Dierkunde*, 43(1):93–112.

Schulte, H. von, and M. de F. Smith
1918. The External Characters, Skeletal Muscles, and Peripheral Nerves of *Kogia breviceps* (Blainville). *Bulletin of the American Museum of Natural History*, 38:7–72.

Simpson, G.G.
1945. The Principles of Classification, and a Classification of Mammals. *Bulletin of the American Museum of Natural History*, 85:1–350.

Sisson, S., and J.D. Grossman
1953. *The Anatomy of the Domestic Animals*. Fourth edition, 972 pages. Philadelphia: W.B. Saunders.

Slijper, E.J.
1979. *Whales*. Second edition, 511 pages. London: Hutchinson. [Translated from the original, *Walvissen*, by A.J. Pomerans.]

Snavely, P.D., N.S. McLeod, W.W. Rau, W.D. Addicott, and J.W. Pearl
1975. Alsea Formation: An Oligocene Marine Sedimentary Sequence in the Oregon Coast Range. *Bulletin of the U.S. Geological Survey*, 1395F:1–21.

Snavely, P.D., N.S. MacLeod, H.C. Wagner, and W.W. Rau
1976. Geology of the Yaquina and Toledo Quadrangles, Oregon. *U.S. Geological Survey, Miscellaneous Investigations Series*, 1:62,500, map I-867:1–21.

Stromer, E.
1908. Die Archaeoceti des ägyptischen Eocäns. *Beiträge zur Geologie und Paläontologie von Österreich-Ungarn*, 21:106–178.

True, F.W.
1907. Remarks on the Type of the Fossil Cetacean *Agorophius pygmaeus* (Müller). *Smithsonian Institution Publication*, 1694:1–8.

Turnbull, W.D.
1970. Mammalian Masticatory Apparatus. *Fieldiana, Geology* 18:147–356.
Vogl, A.W., and H.D. Fisher
1981. The Internal Carotid Artery Does Not Directly Supply the Brain in the Monodontidae (Order Cetacea). *Journal of Morphology,* 170: 207–214.
Whitmore, F.C.
1953. Cranial Morphology of Some Oligocene Artiodactyla. *U.S. Geological Survey Professional Paper,* 243-H:117–160.
Whitmore, F.C., and A.E. Sanders
1977. Review of the Oligocene Cetacea. *Systematic Zoology,* 25:304–320.
Winge, H.
1921. A Review of the Interrelationships of the Cetacea. *Smithsonian Miscellaneous Collections,* 72(8):1–97.
Wood, F.G., and W.E. Evans
1980. Adaptiveness and Ecology of Echolocation in Toothed Whales. *In* R.G. Busnel and J.F. Fish, editors, *Animal Sonar Systems,* pages 381–425. New York: Plenum Press.